INTERNATIONAL JOURNAL FOR NUMERICAL METHODS IN ENGINEERING
Int. J. Numer. Meth. Engng 2013; **94**:221–247
Published online 6 March 2013 in Wiley Online Library (wileyonlinelibrary.com). DOI: 10.1002/nme.4437

Uncertainty quantification of high-dimensional complex systems by multiplicative polynomial dimensional decompositions

Vaibhav Yadav and Sharif Rahman*,†‡

College of Engineering, The University of Iowa, Iowa City, Iowa 52242, USA

SUMMARY

The central theme of this paper is multiplicative polynomial dimensional decomposition (PDD) methods for solving high-dimensional stochastic problems. When a stochastic response is dominantly of multiplicative nature, the standard PDD approximation, predicated on additive function decomposition, may not provide sufficiently accurate probabilistic solutions of a complex system. To circumvent this problem, two multiplicative versions of PDD, referred to as factorized PDD and logarithmic PDD, were developed. Both versions involve a hierarchical, multiplicative decomposition of a multivariate function, a broad range of orthonormal polynomial bases for Fourier-polynomial expansions of component functions, and a dimension-reduction or sampling technique for estimating the expansion coefficients. Three numerical problems involving mathematical functions or uncertain dynamic systems were solved to corroborate how and when a multiplicative PDD is more efficient or accurate than the additive PDD. The results show that indeed, both the factorized and logarithmic PDD approximations can effectively exploit the hidden multiplicative structure of a stochastic response when it exists. Since a multiplicative PDD recycles the same component functions of the additive PDD, no additional cost is incurred. Finally, the random eigensolutions of a sport utility vehicle comprising 40 random variables were evaluated, demonstrating the ability of the new methods to solve industrial-scale problems.

Received 31 January 2012; Revised 6 September 2012; Accepted 20 September 2012

KEY WORDS: ANOVA; dimension reduction; HDMR; random eigenvalue problems; stochastic dynamics

1. INTRODUCTION

Stochastic computing of high-dimensional functions, often defined algorithmically via numerical solution of algebraic, differential, or integral equations, is a vastly expensive and daunting initiative. The fundamental impediment to practical computability is frequently related to the high dimension of the multivariate integration or interpolation problem, known as the curse of dimensionality. The recently invented polynomial dimensional decomposition (PDD) method [1–3] alleviates the curse of dimensionality [4] to some extent by splitting a high-dimensional output function into a finite sum of simpler component functions that are arranged with respect to the degree of interaction among input random variables. In addition, the method exploits the smoothness properties of a stochastic response, whenever possible, by expanding its component functions in terms of measure-consistent orthogonal polynomials, leading to closed-form expressions of the second-moment characteristics of a stochastic solution. Although the same polynomials are extant in polynomial chaos expansion, a recent study found that when the degrees of interaction become progressively weaker or vanish altogether, the PDD approximation commits smaller error than does the polynomial chaos approximation for identical expansion orders [5].

*Correspondence to: Sharif Rahman, Department of Mechanical and Industrial Engineering, The University of Iowa, Iowa City, Iowa 52242, USA.
†E-mail: rahman@engineering.uiowa.edu
‡Professor.

Since PDD stems from the well-known analysis-of-variance (ANOVA) dimensional decomposition [6–12], it is predicated on the additive nature of a function decomposition. This is pertinent as long as the dimensional hierarchy of a stochastic response of interest is also additive. In which case, a truncation of existing PDD, referred to as the additive PDD (A-PDD) in this paper, preserving at most S-variate component functions generates concomitant stochastic solutions with Sth-order polynomial computational complexity. The higher the value of S, the higher the accuracy, but also the computational cost. Based on past work, at least a bivariate A-PDD approximation, that is, selecting $S=2$, is essential for rendering acceptable accuracy in stochastic solutions, with the computational cost varying quadratically with respect to the number of variables [1, 2, 5]. However, the dimensional hierarchy of a stochastic response, in general, is not known *a priori*. Therefore, indiscriminately using A-PDD for general stochastic analysis is not desirable. When a response is dominantly of multiplicative nature, the A-PDD approximation for a chosen truncation parameter S may not predict sufficiently accurate probabilistic characteristics of a complex system. Therefore, alternative decompositions suitable for multiplicative-type response functions and measure-consistent orthogonal polynomials should be explored. For such a decomposition, it is unknown which truncation parameter S should be selected when compared with that for the additive decomposition. Is it possible to solve a stochastic problem by selecting a smaller value of S for the alternative decomposition than for the additive decomposition? In particular, will a univariate PDD method, that is, selecting $S=1$ in the alternative decomposition, provide acceptable accuracy in stochastic solutions, incurring only a linear computational complexity? If yes, then a significant, positive impact on uncertainty quantification of high-dimensional complex systems is anticipated. Further complications may arise when a complex system exhibits a response that is dominantly neither additive nor multiplicative. In the latter case, a mixed approach coupling both additive and multiplicative decompositions, preferably optimally, may be needed. These enhancements, some of which are indispensable, should be pursued without sustaining significant additional cost.

This paper presents two new multiplicative variants of the PDD approximation, referred to as factorized PDD (F-PDD) and logarithmic PDD (L-PDD) approximations, for solving high-dimensional stochastic problems commonly encountered in engineering and applied sciences. The methods are based on (1) hierarchical, multiplicative decompositions of a high-dimensional function in terms of lower-variate component functions, (2) Fourier-polynomial expansions of lower-variate component functions by measure-consistent orthonormal polynomial bases, and (3) dimension-reduction integration or sampling techniques for estimating the expansion coefficients. Section 2 formally defines a general stochastic problem, followed by the ANOVA dimensional decomposition of a multivariate function. Section 3 briefly explains how ANOVA leads up to A-PDD approximation, an existing stochastic method. A multiplicative dimensional decomposition, including a proof of existence and uniqueness, is presented in Section 4. In addition, the section reveals the relationship or similarity among A-PDD, F-PDD, and L-PDD, establishing how the latter two methods can exploit a hidden multiplicative structure, if it exists, of a stochastic response. The calculation of the expansion coefficients by dimension-reduction integration and sampling techniques is described in Section 5. Section 6 presents three numerical examples involving mathematical functions or random eigenvalue problems, contrasting the accuracy, convergence properties, and computational efforts of the proposed and existing methods. A large-scale stochastic-dynamics problem, solved using the new PDD methods, is reported in Section 7. Finally, conclusions are drawn in Section 8.

2. ANOVA DIMENSIONAL DECOMPOSITION

Let $\mathbb{N}$, $\mathbb{N}_0$, $\mathbb{R}$, and $\mathbb{R}_0^+$ represent the sets of positive integer (natural), nonnegative integer, real, and nonnegative real numbers, respectively. For $k \in \mathbb{N}$, denote by $\mathbb{R}^k$ the k-dimensional Euclidean space, by $\mathbb{N}_0^k$ the k-dimensional multi-index space, and by $\mathbb{R}^{k\times k}$ the set of $k\times k$ real-valued matrices. These standard notations will be used throughout the paper.

Let $(\Omega, \mathcal{F}, P)$ be a complete probability space, where Ω is a sample space, $\mathcal{F}$ is a σ-field on Ω, and $P : \mathcal{F} \to [0, 1]$ is a probability measure. With $\mathcal{B}^N$ representing the Borel σ-field on $\mathbb{R}^N$, $N \in \mathbb{N}$, consider an $\mathbb{R}^N$-valued random vector $\mathbf{X} := (X_1, \ldots, X_N) : (\Omega, \mathcal{F}) \to (\mathbb{R}^N, \mathcal{B}^N)$,

DOI: 10.1002/nme

which describes the statistical uncertainties in all system and input parameters of a high-dimensional stochastic problem. The probability law of $\mathbf{X}$ is completely defined by its joint probability density function $f_{\mathbf{X}} : \mathbb{R}^N \to \mathbb{R}_0^+$. Assuming independent coordinates of $\mathbf{X}$, its joint probability density $f_{\mathbf{X}}(\mathbf{x}) = \Pi_{i=1}^{i=N} f_i(x_i)$ is expressed by a product of marginal probability density functions f_i of X_i, $i = 1, \ldots, N$, defined on the probability triple $(\Omega_i, \mathcal{F}_i, P_i)$ with a bounded or an unbounded support on $\mathbb{R}$. For a given $u \subseteq \{1, \ldots, N\}$, $f_{\mathbf{X}_{-u}}(\mathbf{x}_{-u}) := \prod_{i=1, i\notin u}^{N} f_i(x_i)$ defines the marginal density function of $\mathbf{X}_{-u} := \mathbf{X}_{\{1,\ldots,N\}\setminus u}$.

Let $y(\mathbf{X}) := y(X_1, \ldots, X_N)$, a real-valued, measurable transformation on $(\Omega, \mathcal{F})$, define a high-dimensional stochastic response of interest and $\mathcal{L}_2(\Omega, \mathcal{F}, P)$ a Hilbert space of square-integrable functions y with respect to the induced generic measure $f_{\mathbf{X}}(\mathbf{x})d\mathbf{x}$ supported on $\mathbb{R}^N$. The ANOVA dimensional decomposition, expressed by the recursive form [7, 11, 12]

$$y(\mathbf{X}) = \sum_{u\subseteq\{1,\ldots,N\}} y_u(\mathbf{X}_u), \tag{1}$$

$$y_\emptyset = \int_{\mathbb{R}^N} y(\mathbf{x}) f_{\mathbf{X}}(\mathbf{x}) \mathrm{d}\mathbf{x}, \tag{2}$$

$$y_u(\mathbf{X}_u) = \int_{\mathbb{R}^{N-|u|}} y(\mathbf{X}_u, \mathbf{x}_{-u}) f_{\mathbf{X}_{-u}}(\mathbf{x}_{-u}) \mathrm{d}\mathbf{x}_{-u} - \sum_{v\subset u} y_v(\mathbf{X}_v), \tag{3}$$

is a finite, hierarchical expansion in terms of its input variables with increasing dimensions, where $u \subseteq \{1, \ldots, N\}$ is a subset with the complementary set $-u = \{1, \ldots, N\}\setminus u$ and cardinality $0 \leqslant |u| \leqslant N$, and y_u is a $|u|$-variate component function describing a constant or the interactive effect of $\mathbf{X}_u = (X_{i_1}, \ldots, X_{i_{|u|}})$, $1 \leqslant i_1 < \cdots < i_{|u|} \leqslant N$, a subvector of $\mathbf{X}$, on y when $|u| = 0$ or $|u| > 0$. The summation in Equation (1) comprises 2^N terms, with each term depending on a group of variables indexed by a particular subset of $\{1, \ldots, N\}$, including the empty set $\emptyset$. In Equation (3), $(\mathbf{X}_u, \mathbf{x}_{-u})$ denotes an N-dimensional vector whose ith component is X_i if $i \in u$ and x_i if $i \notin u$. When $u = \emptyset$, the sum in Equation (3) vanishes, resulting in the expression of the constant function $y_\emptyset$ in Equation (2). When $u = \{1, \ldots, N\}$, the integration in Equation (3) is on the empty set, reproducing Equation (1) and hence finding the last function $y_{\{1,\ldots,N\}}$. Indeed, all component functions of y can be obtained by interpreting literally Equation (3). On inversion, Equations (1)–(3) result in [11, 12]

$$y(\mathbf{X}) = \sum_{u\subseteq\{1,\ldots,N\}} \sum_{v\subseteq u} (-1)^{|u|-|v|} \int_{\mathbb{R}^{N-|v|}} y(\mathbf{X}_v, \mathbf{x}_{-v}) f_{\mathbf{X}_{-v}}(\mathbf{x}_{-v}) \mathrm{d}\mathbf{x}_{-v}, \tag{4}$$

providing an explicit form of the same decomposition.

Remark 1

The ANOVA component functions y_u, $u \subseteq \{1, \ldots, N\}$, are uniquely determined from the annihilating conditions [7, 11, 12]

$$\int_{\mathbb{R}} y_u(\mathbf{x}_u) f_i(x_i) \mathrm{d}x_i = 0 \text{ for } i \in u, \tag{5}$$

resulting in two remarkable properties: (1) the component functions, y_u, $\emptyset \neq u \subseteq \{1, \ldots, N\}$, have zero means; and (2) two distinct component functions y_u and y_v, where $u \subseteq \{1, \ldots, N\}$, $v \subseteq \{1, \ldots, N\}$, and $u \neq v$, are orthogonal. Further details are available elsewhere [12].

Remark 2

Traditionally, Equations (1)–(3) or (4) with X_j, $j = 1, \ldots, N$, following independent, standard uniform distributions, are identified as the ANOVA decomposition [7, 11]; however, recent works reveal no fundamental requirement for a specific probability measure of $\mathbf{X}$, provided that the resultant

DOI: 10.1002/nme

integrals in Equations (1)–(3) or (4) exist and are finite [1, 2, 12]. In this work, the ANOVA dimensional decomposition should be interpreted with respect to an arbitrary but product type probability measure for which it is always endowed with desirable orthogonal properties.

Remark 3
The nonconstant component functions of the classical or standard ANOVA decomposition, described by Equation (3), are applicable for independent coordinates of $\mathbf{X}$. For statistically dependent variables, a unique ANOVA decomposition also exists, although subject to mild restrictive conditions. In which case, Equation (3) must be generalized to account for nonproduct type probability measures. The authors do not pursue it here.

3. ADDITIVE POLYNOMIAL DIMENSIONAL DECOMPOSITION

Let $\{\psi_{ij}(X_i);\ j = 0, 1, \ldots\}$ be a set of orthonormal polynomial basis functions in the Hilbert space $\mathcal{L}_2(\Omega_i, \mathcal{F}_i, P_i)$ that is consistent with the probability measure P_i of X_i. For a given $\emptyset \neq u = \{i_1, \ldots, i_{|u|}\} \subseteq \{1, \ldots, N\}$, $1 \leqslant |u| \leqslant N$, $1 \leqslant i_1 < \cdots < i_{|u|} \leqslant N$, denote a product probability triple by $\left(\times_{p=1}^{p=|u|}\Omega_{i_p}, \times_{p=1}^{p=|u|}\mathcal{F}_{i_p}, \times_{p=1}^{p=|u|}P_{i_p}\right)$, and the associated space of square-integrable $|u|$-variate component functions of y by $\mathcal{L}_2\left(\times_{p=1}^{p=|u|}\Omega_{i_p}, \times_{p=1}^{p=|u|}\mathcal{F}_{i_p}, \times_{p=1}^{p=|u|}P_{i_p}\right) := \left\{y_u : \int_{\mathbb{R}^{|u|}} y_u^2(\mathbf{x}_u) f_{\mathbf{X}_u}(\mathbf{x}_u)\mathrm{d}\mathbf{x}_u < \infty\right\}$, which is a Hilbert space. Since the joint density of $(X_{i_1}, \ldots, X_{i_{|u|}})$ is separable (independence), that is, $f_{\mathbf{X}_u}(\mathbf{x}_u) = \prod_{p=1}^{|u|} f_{i_p}\left(x_{i_p}\right)$, the product polynomial $\psi_{u\mathbf{j}_{|u|}}(\mathbf{X}_u) := \prod_{p=1}^{|u|}\psi_{i_p j_p}\left(X_{i_p}\right)$, where $\mathbf{j}_{|u|} = (j_1, \ldots, j_{|u|}) \in \mathbb{N}_0^{|u|}$, a $|u|$-dimensional multi-index with ∞-norm $\left\|\mathbf{j}_{|u|}\right\|_\infty = \max(j_1, \ldots, j_{|u|})$, constitutes an orthonormal basis in $\mathcal{L}_2\left(\times_{p=1}^{p=|u|}\Omega_{i_p}, \times_{p=1}^{p=|u|}\mathcal{F}_{i_p}, \times_{p=1}^{p=|u|}P_{i_p}\right)$. Two important properties of these product polynomials from the tensor product of Hilbert spaces are as follows.

Proposition 4
The product polynomials $\psi_{u\mathbf{j}_{|u|}}(\mathbf{X}_u)$, $\emptyset \neq u \subseteq \{1, \ldots, N\}$, $j_1, \cdots, j_{|u|} \neq 0$, have *zero* means, that is,

$$\mathbb{E}\left[\psi_{u\mathbf{j}_{|u|}}(\mathbf{X}_u)\right] = 0. \tag{6}$$

Proposition 5
Two distinct product polynomials $\psi_{u\mathbf{j}_{|u|}}(\mathbf{X}_u)$ and $\psi_{vk_{|v|}}(\mathbf{X}_v)$, where $\emptyset \neq u \subseteq \{1, \ldots, N\}$, $\emptyset \neq v \subseteq \{1, \ldots, N\}$, $j_1, \cdots, j_{|u|} \neq 0$, $k_1, \cdots, k_{|v|} \neq 0$, are uncorrelated, and each has unit variance, that is,

$$\mathbb{E}\left[\psi_{u\mathbf{j}_{|u|}}(\mathbf{X}_u)\psi_{vk_{|v|}}(\mathbf{X}_v)\right] = \begin{cases} 1 & \text{if } u = v; \mathbf{j}_{|u|} = \mathbf{k}_{|v|}, \\ 0 & \text{otherwise.} \end{cases} \tag{7}$$

Proof
The results of Propositions 4 and 5 follow by recognizing independent coordinates of $\mathbf{X}$ and using the second-moment properties of univariate orthonormal polynomials: (1) $\mathbb{E}[\psi_{ij}(X_i)] = 1$ when $j = 0$ and *zero* when $j \geqslant 1$; (2) $\mathbb{E}\left[\psi_{ij_1}(X_i)\psi_{ij_2}(X_i)\right] = 1$ when $j_1 = j_2$ and *zero* when $j_1 \neq j_2$ for an arbitrary random variable X_i, where $\mathbb{E}$ is the expectation operator with respect to the probability measure $f_{\mathbf{X}}(\mathbf{x})d\mathbf{x}$. □

As a result, the orthogonal polynomial expansion of a nonconstant $|u|$-variate component function becomes [1, 2]

$$y_u(\mathbf{X}_u) = \sum_{\substack{\mathbf{j}_{|u|} \in \mathbb{N}_0^{|u|} \\ j_1, \ldots, j_{|u|} \neq 0}} C_{u\mathbf{j}_{|u|}}\psi_{u\mathbf{j}_{|u|}}(\mathbf{X}_u),\ \emptyset \neq u \subseteq \{1, \ldots, N\}, \tag{8}$$

DOI: 10.1002/nme

with

$$C_{u\mathbf{j}_{|u|}} := \int_{\mathbb{R}^N} y(\mathbf{x})\psi_{u\mathbf{j}_{|u|}}(\mathbf{x}_u) f_{\mathbf{X}}(\mathbf{x})\mathrm{d}\mathbf{x} \tag{9}$$

representing the corresponding expansion coefficient. For instance, when $u = \{i\}$, $i = 1, \ldots, N$, the univariate component functions and expansion coefficients are $y_{\{i\}}(X_i) = \sum_{j=1}^{\infty} C_{ij}\psi_{ij}(X_i)$ and $C_{ij} := C_{\{i\}(j)}$, respectively. Using Propositions 4 and 5, all component functions y_u, $\emptyset \neq u \subseteq \{1, \ldots, N\}$, are found to satisfy the annihilating conditions of the ANOVA dimensional decomposition. The end result of combining Equations (1) and (8) is the additive PDD [1, 2]

$$y(\mathbf{X}) = y_\emptyset + \sum_{\emptyset \neq u \subseteq \{1,\ldots,N\}} \sum_{\substack{\mathbf{j}_{|u|} \in \mathbb{N}_0^{|u|} \\ j_1,\ldots,j_{|u|} \neq 0}} C_{u\mathbf{j}_{|u|}} \psi_{u\mathbf{j}_{|u|}}(\mathbf{X}_u), \tag{10}$$

providing an exact, hierarchical expansion of y in terms of an infinite number of coefficients or orthonormal polynomials. In practice, the number of coefficients or polynomials must be finite, say, by retaining at most mth-order polynomials in each variable. Furthermore, in many applications, the function y can be approximated by a sum of at most S-variate component functions, where $1 \leqslant S \leqslant N$, resulting in the S-variate, mth-order A-PDD approximation

$$\tilde{y}_{S,m}(\mathbf{X}) = y_\emptyset + \sum_{\substack{\emptyset \neq u \subseteq \{1,\ldots,N\} \\ 1 \leqslant |u| \leqslant S}} \sum_{\substack{\mathbf{j}_{|u|} \in \mathbb{N}_0^{|u|}, \left\|\mathbf{j}_{|u|}\right\|_\infty \leqslant m \\ j_1,\ldots,j_{|u|} \neq 0}} C_{u\mathbf{j}_{|u|}} \psi_{u\mathbf{j}_{|u|}}(\mathbf{X}_u), \tag{11}$$

containing $\sum_{k=0}^{S} \binom{N}{S-k} m^{S-k}$ number of PDD coefficients and corresponding orthonormal polynomials. Due to its additive structure, the approximation in Equation (11) includes degrees of interaction among at most S input variables $X_{i_1}, \ldots, X_{i_S}$, $1 \leqslant i_1 \leqslant \cdots \leqslant i_S \leqslant N$. For instance, by selecting $S = 1$ and 2, the functions $\tilde{y}_{1,m}$ and $\tilde{y}_{2,m}$ respectively provide univariate and bivariate mth-order approximations, contain contributions from all input variables, and should not be viewed as first-order and second-order approximations, nor do they limit the nonlinearity of y. Depending on how the component functions are constructed, arbitrarily high-order univariate and bivariate terms of y could be lurking inside $\tilde{y}_{1,m}$ and $\tilde{y}_{2,m}$. When $S \to N$ and $m \to \infty$, $\tilde{y}_{S,m}$ converges to y in the mean-square sense, permitting Equation (11) to generate a hierarchical and convergent sequence of approximations of y.

Applying the expectation operator on $\tilde{y}_{S,m}(\mathbf{X})$ and $(\tilde{y}_{S,m}(\mathbf{X}) - y_\emptyset)^2$ and noting Propositions 4 and 5, the mean [3]

$$\mathbb{E}[\tilde{y}_{S,m}(\mathbf{X})] = y_\emptyset \tag{12}$$

of the S-variate, mth-order PDD approximation matches the exact mean $\mathbb{E}[y(\mathbf{X})]$, regardless of S or m, and the approximate variance [3]

$$\mathbb{E}\left[(\tilde{y}_{S,m}(\mathbf{X}) - \mathbb{E}[\tilde{y}_{S,m}(\mathbf{X})])^2\right] = \sum_{\substack{\emptyset \neq u \subseteq \{1,\ldots,N\} \\ 1 \leqslant |u| \leqslant S}} \sum_{\substack{\mathbf{j}_{|u|} \in \mathbb{N}_0^{|u|}, \left\|\mathbf{j}_{|u|}\right\|_\infty \leqslant m \\ j_1,\ldots,j_{|u|} \neq 0}} C^2_{u\mathbf{j}_{|u|}} \tag{13}$$

is calculated as the sum of squares of the expansion coefficients from the S-variate, mth-order A-PDD approximation of $y(\mathbf{X})$. A recent work proved that the approximate variance in Equation (13) approaches the exact variance of y when $S \to N$ and $m \to \infty$ [3]. The mean-square convergence of $\tilde{y}_{S,m}$ is guaranteed as y, and its component functions are all members of the associated Hilbert spaces.

For the special case of $S = 1$, the univariate A-PDD approximation

$$\tilde{y}_{1,m}(\mathbf{X}) = y_\emptyset + \sum_{i=1}^{N} \sum_{j=1}^{m} C_{ij}\psi_{ij}(X_i) \tag{14}$$

DOI: 10.1002/nme

of $y(\boldsymbol{X})$ yields the exact mean

$$\mathbb{E}[\tilde{y}_{1,m}(\mathbf{X})] = y_{\emptyset} \tag{15}$$

and an approximate variance

$$\mathbb{E}\left[(\tilde{y}_{1,m}(\mathbf{X}) - \mathbb{E}[\tilde{y}_{1,m}(\mathbf{X})])^2\right] = \sum_{i=1}^{N}\sum_{j=1}^{m} C_{ij}^2 \tag{16}$$

that depends on $m < \infty$.

4. PROPOSED MULTIPLICATIVE POLYNOMIAL DIMENSIONAL DECOMPOSITIONS

4.1. Multiplicative function decomposition

Consider a general multiplicative form

$$y(\mathbf{X}) = \prod_{u \subseteq \{1,\ldots,N\}} [1 + z_u(\mathbf{X}_u)] \tag{17}$$

of the dimensional decomposition of y, where z_u, $u \subseteq \{1,\ldots,N\}$, are various component functions of input variables with increasing dimensions. Like the sum in Equation (1), the product in Equation (17) comprises 2^N terms, with each term depending on a group of variables indexed by a particular subset of $\{1,\ldots,N\}$, including the empty set $\emptyset$. Tunga and Demiralp [13] originally proposed this decomposition, calling it factorized high-dimensional model representation. However, it is not obvious if such decomposition exists uniquely for a general multivariate function y. Lemma 6 and Theorem 7 demonstrate that, indeed, it does with some restrictions.

Lemma 6
The ANOVA component functions y_v, $v \subseteq \{1,\ldots,N\}$, of a square-integrable function $y : \mathbb{R}^N \to \mathbb{R}$, when integrated with respect to the probability measure $f_{\mathbf{X}_{-u}}(\mathbf{x}_{-u})\mathrm{d}\mathbf{x}_{-u} = \prod_{i=1,i\notin u}^{N} f_i(x_i)\mathrm{d}x_i$, $u \subseteq \{1,\ldots,N\}$, satisfy

$$\int_{\mathbb{R}^{N-|u|}} y_v(\mathbf{x}_v) f_{\mathbf{X}_{-u}}(\mathbf{x}_{-u})\mathrm{d}\mathbf{x}_{-u} = \begin{cases} y_v(\mathbf{x}_v) & \text{if } v \subseteq u, \\ 0 & \text{if } v \not\subseteq u. \end{cases} \tag{18}$$

Proof
For any two subsets $v \subseteq \{1,\ldots,N\}$, $u \subseteq \{1,\ldots,N\}$, $(v \cap -u) \subseteq -u$ and $-u = (-u \setminus (v \cap -u)) \cup (v \cap -u)$. If $v \subseteq u$, then $y_v(\mathbf{x}_v)$ does not depend on $\mathbf{x}_{-u}$, resulting in

$$\int_{\mathbb{R}^{N-|u|}} y_v(\mathbf{x}_v) f_{\mathbf{X}_{-u}}(\mathbf{x}_{-u})\mathrm{d}\mathbf{x}_{-u} = y_v(\mathbf{x}_v)\int_{\mathbb{R}^{N-|u|}} f_{\mathbf{X}_{-u}}(\mathbf{x}_{-u})\mathrm{d}\mathbf{x}_{-u} = y_v(\mathbf{x}_v), \tag{19}$$

the nontrivial result of Equation (18). When $v \not\subseteq u$, consider an integer $k \in (v \cap -u)$, so that $k \in v$. Then

$$\begin{aligned}
\int_{\mathbb{R}^{N-|u|}} y_v(\mathbf{x}_v) f_{\mathbf{X}_{-u}}(\mathbf{x}_{-u})\mathrm{d}\mathbf{x}_{-u} &= \int_{\mathbb{R}^{N-|u|-|v\cap -u|}} \int_{\mathbb{R}^{|v\cap -u|}} y_v(\mathbf{x}_v) f_{\mathbf{X}_{-u}}(\mathbf{x}_{-u})\mathrm{d}\mathbf{x}_{v\cap -u}\mathrm{d}\mathbf{x}_{-u\setminus(v\cap -u)} \\
&= \int_{\mathbb{R}^{N-|u|-|v\cap -u|-1}} \left(\int_{\mathbb{R}} y_v(\mathbf{x}_v) f_k(x_k)\mathrm{d}x_k\right) \\
&\quad \times \prod_{j\in(v\cap -u), j\neq k} f_j(x_j)\mathrm{d}\mathbf{x}_{(v\cap -u)\setminus\{k\}}\mathrm{d}\mathbf{x}_{-u\setminus(v\cap -u)} \\
&= 0,
\end{aligned} \tag{20}$$

where the equality to *zero* in the last line follows from using Equation (5). □

DOI: 10.1002/nme

Theorem 7
A square-integrable function $y : \mathbb{R}^N \to \mathbb{R}$ for a given probability measure $f_{\mathbf{X}}(\mathbf{x})\mathrm{d}\mathbf{x} = \Pi_{i=1}^{i=N} f_i(x_i)dx_i$ admits a unique multiplicative dimensional decomposition expressed by Equation (17).

Proof
Changing the dummy index from u to v, replacing $\mathbf{X}$ with $\mathbf{x}$, and integrating both sides of Equation (1) with respect to the measure $f_{\mathbf{X}_{-u}}(\mathbf{x}_{-u})\mathrm{d}\mathbf{x}_{-u}$, that is, over all variables except $\mathbf{x}_u$, yields

$$\int_{\mathbb{R}^{N-|u|}} y(\mathbf{x}) f_{\mathbf{X}_{-u}}(\mathbf{x}_{-u})\mathrm{d}\mathbf{x}_{-u} = \sum_{v\subseteq\{1,\ldots,N\}} \int_{\mathbb{R}^{N-|u|}} y_v(\mathbf{x}_v) f_{\mathbf{X}_{-u}}(\mathbf{x}_{-u})\mathrm{d}\mathbf{x}_{-u}. \tag{21}$$

Using Lemma 6, Equation (21) simplifies to

$$\int_{\mathbb{R}^{N-|u|}} y(\mathbf{x}) f_{\mathbf{X}_{-u}}(\mathbf{x}_{-u})\mathrm{d}\mathbf{x}_{-u} = \sum_{v\subseteq u} y_v(\mathbf{x}_v) = y_u(\mathbf{x}_u) + \sum_{v\subset u} y_v(\mathbf{x}_v) \tag{22}$$

with $\subset$ representing proper subset (strict inclusion). Therefore, for any $u \subseteq \{1,\ldots,N\}$, including $\emptyset$,

$$y_u(\mathbf{x}_u) = \int_{\mathbb{R}^{N-|u|}} y(\mathbf{x}) f_{\mathbf{X}_{-u}}(\mathbf{x}_{-u})\mathrm{d}\mathbf{x}_{-u} - \sum_{v\subset u} y_v(\mathbf{x}_v), \tag{23}$$

proving the existence and uniqueness of ANOVA component functions for a square-integrable function. To do the same for the multiplicative component functions, expand the right side of Equation (17) to form

$$\begin{aligned} y(\mathbf{X}) = z_\emptyset + &\sum_{\substack{u\subseteq\{1,\ldots,N\}\\|u|=1}} r_u(z_v(\mathbf{X}_v); v\subseteq u) + \sum_{\substack{u\subseteq\{1,\ldots,N\}\\|u|=2}} r_u(z_v(\mathbf{X}_v); v\subseteq u) + \cdots \\ &+ r_{\{1,\ldots,N\}}(z_v(\mathbf{X}_v); v\subseteq\{1,\ldots,N\}) \\ = &\sum_{u\subseteq\{1,\ldots,N\}} r_u(z_v(\mathbf{X}_v); v\subseteq u), \end{aligned} \tag{24}$$

where $r_u(z_v(\mathbf{X}_v); v \subseteq u)$ is a function of at most $|u|$-variate multiplicative component functions of y. For instance, when $u = \emptyset$, $u = \{i\}$, and $u = \{i_1, i_2\}$, $i, i_1, i_2 = 1,\ldots,N$, $i_2 > i_1$, the corresponding r_u-functions are $r_\emptyset(z_\emptyset) = z_\emptyset$, $r_{\{i\}}(z_\emptyset, z_{\{i\}}(X_i))$, and $r_{\{i_1,i_2\}}(z_\emptyset, z_{\{i_1\}}(X_{i_1}), z_{\{i_2\}}(X_{i_2}), z_{\{i_1,i_2\}}(X_{i_1}, X_{i_2}))$, respectively. Comparing Equations (1) and (24) yields the recursive relationship,

$$r_u(z_v(\mathbf{X}_v); v\subseteq u) = y_u(\mathbf{X}_u), \tag{25}$$

which, on inversion, expresses $z_u, u \subseteq \{1,\ldots N\}$, in terms of the additive ANOVA component functions $y_v, v \subseteq u$. Therefore, given a probability measure of $\mathbf{X}$, the functions r_u and $z_u, u \subseteq \{1,\ldots N\}$, also exist and are unique. □

In this work, two new multiplicative PDDs, referred to as factorized PDD and logarithmic PDD, were developed in the spirit of additive PDD for tackling high-dimensional stochastic response functions endowed with multiplicative dimensional hierarchies. Both decompositions, rooted in Equation (17), exploit the smoothness properties of a stochastic solution, if they exist, by measure-consistent orthogonal polynomials, and are described in the following subsections.

DOI: 10.1002/nme

4.2. Factorized polynomial dimensional decomposition

The F-PDD is built on two principal steps: (1) finding the explicit relationships between the component functions of the ANOVA and the multiplicative dimensional decompositions of a multivariate function y, and (2) expanding the ANOVA component functions in terms of the measure-consistent orthonormal polynomial basis functions. Theorem 8 reveals the desired relationships in the first step.

Theorem 8
The recursive relationships between component functions of the ANOVA and multiplicative dimensional decompositions of a square-integrable function $y : \mathbb{R}^N \to \mathbb{R}$, represented by Equations (1) and (17), respectively, are

$$1 + z_u(\mathbf{X}_u) = \frac{\sum_{v \subseteq u} y_v(\mathbf{X}_v)}{\prod_{v \subset u} [1 + z_v(\mathbf{X}_v)]}, \; u \subseteq \{1, \ldots, N\}. \tag{26}$$

Proof
Since Equations (1) and (17) represent the same function y,

$$\sum_{u \subseteq \{1,\ldots,N\}} y_u(\mathbf{X}_u) = \prod_{u \subseteq \{1,\ldots,N\}} [1 + z_u(\mathbf{X}_u)], \tag{27}$$

which, as is, is unwieldy to solve for z_u. However, from Equation (25), the solution z_u for $u \subseteq \{1, \ldots, N\}$ depends only on functions y_v such that $v \subseteq u$. Therefore, all remaining additive or multiplicative component functions not involved can be assigned arbitrary values. In particular, setting $y_v = z_v = 0$ for all $v \not\subseteq u$ in Equation (27) results in

$$\sum_{v \subseteq u} y_v(\mathbf{X}_v) = \prod_{v \subseteq u} [1 + z_v(\mathbf{X}_v)] = [1 + z_u(\mathbf{X}_u)] \prod_{v \subset u} [1 + z_v(\mathbf{X}_v)], \tag{28}$$

which, on inversion, yields Equation (26), completing the proof. □

Corollary 9
Recursive evaluations of Equation (26) eliminate $1 + z_v$, $v \subset u$, leading to an explicit form of

$$1 + z_u(\mathbf{X}_u) = \cfrac{\sum_{w_{|u|} \subseteq u} y_{w_{|u|}}\left(\mathbf{X}_{w_{|u|}}\right)}{\prod_{w_{|u|} \subset u} \cfrac{\sum_{w_{|u|-1} \subseteq w_{|u|}} y_{w_{|u|-1}}\left(\mathbf{X}_{w_{|u|-1}}\right)}{\prod_{w_{|u|-1} \subset w_{|u|}} \cfrac{\ddots}{\ddots \prod_{w_2 \subset w_3} \cfrac{\sum_{w_1 \subseteq w_2} y_{w_1}(\mathbf{X}_{w_1})}{\prod_{w_1 \subset w_2} \cfrac{\sum_{w_0 \subseteq w_1} y_{w_0}(\mathbf{X}_{w_0})}{1}}}}} \tag{29}$$

for any $u \subseteq \{1, \ldots, N\}$, solely in terms of the ANOVA component functions.

Corollary 10
The multiplicative constant, univariate, and bivariate component functions of a square-integrable function $y : \mathbb{R}^N \to \mathbb{R}$, obtained by setting $u = \emptyset$, $u = \{i\}$; $i = 1, \ldots, N$, and $u = \{i_1, i_2\}$; $i_1 < i_2 = 1, \ldots, N$, respectively, in Equation (26) or (29) are

$$1 + z_\emptyset = y_\emptyset, \tag{30}$$

DOI: 10.1002/nme

$$1 + z_{\{i\}}(X_i) = \frac{y_\emptyset + y_{\{i\}}(X_i)}{y_\emptyset}, \tag{31}$$

and

$$1 + z_{\{i_1,i_2\}}(X_{i_1}, X_{i_2}) = \frac{y_\emptyset + y_{\{i_1\}}(X_{i_1}) + y_{\{i_2\}}(X_{i_2}) + y_{\{i_1,i_2\}}(X_{i_1}, X_{i_2})}{y_\emptyset\left[\dfrac{y_\emptyset + y_{\{i_1\}}(X_{i_1})}{y_\emptyset}\right]\left[\dfrac{y_\emptyset + y_{\{i_2\}}(X_{i_2})}{y_\emptyset}\right]}. \tag{32}$$

Remark 11
Equations (30) – (32) can also be obtained employing the identity and first-degree and second-degree idempotent operators [13]. However, to obtain similar expressions for trivariate and higher-variate multiplicative component functions, an extensive amount of algebra associated with third-degree and higher-degree idempotent operators will be required. This is the primary reason why component functions with three or more variables have yet to be reported in the current literature. Theorem 8, in contrast, is simpler and, more importantly, provides a general expression – Equation (26) or (29) – that is valid for a multiplicative component function of an arbitrary number of variables.

The next step entails representing the ANOVA component functions by their Fourier-polynomial expansions, that is, applying Equation (8) into Equation (26), which results in expressing the multiplicative component functions

$$1 + z_u(\mathbf{X}_u) = \frac{y_\emptyset + \displaystyle\sum_{\emptyset \neq v \subseteq u} \sum_{\substack{\mathbf{j}_{|v|} \in \mathbb{N}_0^{|v|} \\ j_1,\ldots,j_{|v|} \neq 0}} C_{v\mathbf{j}_{|v|}} \psi_{v\mathbf{j}_{|v|}}(\mathbf{X}_v)}{\displaystyle\prod_{v \subset u} [1 + z_v(\mathbf{X}_v)]}, \quad u \subseteq \{1, \ldots, N\}, \tag{33}$$

in terms of orthonormal polynomials as well. Finally, combining Equations (17) and (33) creates the F-PDD of

$$y(\mathbf{X}) = y_\emptyset \prod_{\emptyset \neq u \subseteq \{1,\ldots,N\}} \left[\frac{y_\emptyset + \displaystyle\sum_{\emptyset \neq v \subseteq u} \sum_{\substack{\mathbf{j}_{|v|} \in \mathbb{N}_0^{|v|} \\ j_1,\ldots,j_{|v|} \neq 0}} C_{v\mathbf{j}_{|v|}} \psi_{v\mathbf{j}_{|v|}}(\mathbf{X}_v)}{\displaystyle\prod_{v \subset u} [1 + z_v(\mathbf{X}_v)]} \right], \tag{34}$$

also an exact representation of $y(\mathbf{X})$, where infinite orthonormal polynomials of increasing dimensions are structured with a multiplicative hierarchy, as opposed to the additive hierarchy in Equation (10). Consequently, an S-variate, mth-order F-PDD approximation, retaining at most S-variate component functions and mth-order orthogonal polynomials, becomes

$$\hat{y}_{S,m}(\mathbf{X}) = y_\emptyset \prod_{\substack{\emptyset \neq u \subseteq \{1,\ldots,N\} \\ 1 \leqslant |u| \leqslant S}} \left[\frac{y_\emptyset + \displaystyle\sum_{\emptyset \neq v \subseteq u} \sum_{\substack{\mathbf{j}_{|v|} \in \mathbb{N}_0^{|v|}, \|\mathbf{j}_{|u|}\|_\infty \leqslant m \\ j_1,\ldots,j_{|v|} \neq 0}} C_{v\mathbf{j}_{|v|}} \psi_{v\mathbf{j}_{|v|}}(\mathbf{X}_v)}{\displaystyle\prod_{v \subset u} [1 + z_v(\mathbf{X}_v)]} \right]. \tag{35}$$

It is elementary to show that the S-variate, mth-order F-PDD approximation converges to $y(\mathbf{X})$ in the mean-square sense when $S \to N$ and $m \to \infty$. It is worth noting that Equations (33)–(35) can also be expressed explicitly, solely in terms of orthonormal polynomials exploiting Equation (29). However, they are not reported here because of their more complicated form.

Although the right side of Equation (35) contains products of at most S univariate polynomials, no simple expressions are available for the second-moment properties of $\hat{y}_{S,m}(\mathbf{X})$ if S and

DOI: 10.1002/nme

m are selected arbitrarily. However, any probabilistic characteristic of $y(\mathbf{X})$ is easily estimated by the Monte Carlo simulation (MCS) of $\hat{y}_{S,m}(\mathbf{X})$ in Equation (35). When $S = 1$, the univariate F-PDD approximation

$$\hat{y}_{1,m}(\mathbf{X}) = y_{\emptyset}\left[\prod_{i=1}^{N}\left\{1 + \frac{1}{y_{\emptyset}}\sum_{j=1}^{m} C_{ij}\,\psi_{ij}(X_i)\right\}\right] \tag{36}$$

forms a product of univariate polynomials, guiding to closed-form expressions of its second-moment properties. Indeed, it is elementary to show that Equation (36) results in the exact mean

$$\mathbb{E}[\hat{y}_{1,m}(\mathbf{X})] = y_{\emptyset}, \tag{37}$$

but an approximate variance

$$\mathbb{E}[(\hat{y}_{1,m}(\mathbf{X}) - \mathbb{E}\left[\hat{y}_{1,m}(\mathbf{X})\right])^2] = y_{\emptyset}^2\left[\prod_{i=1}^{N}\left(1 + \frac{1}{y_{\emptyset}^2}\sum_{j=1}^{m} C_{ij}^2\right) - 1\right] \tag{38}$$

that are valid for an arbitrary $m < \infty$.

4.3. Logarithmic polynomial dimensional decomposition

The L-PDD is constructed by invoking the ANOVA dimensional decomposition of the logarithmic transformation of a stochastic response, followed by the Fourier-polynomial expansions of the ANOVA component functions in terms of the measure-consistent orthonormal polynomial basis functions.

The ANOVA dimensional decomposition of the logarithm of a stochastic response $w(\boldsymbol{X}) := \ln y(\boldsymbol{X})$, if it exists, is

$$w(\mathbf{X}) = \sum_{u \subseteq \{1,\ldots,N\}} w_u(\mathbf{X}_u), \tag{39}$$

$$w_{\emptyset} = \int_{\mathbb{R}^N} \ln y(\mathbf{x})\, f_{\mathbf{X}}(\mathbf{x})\mathrm{d}\mathbf{x}, \tag{40}$$

$$w_u(\mathbf{X}_u) = \int_{\mathbb{R}^{N-|u|}} \ln y(\mathbf{X}_u, \mathbf{x}_{-u})\, f_{\mathbf{X}_{-u}}(\mathbf{x}_{-u})\mathrm{d}\mathbf{x}_{-u} - \sum_{v \subset u} w_v(\mathbf{X}_v), \tag{41}$$

where w_u is a $|u|$-variate component function describing a constant or the interactive effect of $\mathbf{X}_u$ on w when $|u| = 0$ or $|u| > 0$. On exponentiation, Equation (39) reverts to

$$y(\mathbf{X}) = \prod_{u \subseteq \{1,\ldots,N\}} \exp[w_u(\mathbf{X}_u)], \tag{42}$$

an expansion of the original function. Compared with Equation (17), Equation (42) represents another multiplicative dimensional decomposition when $\exp[w_u(\mathbf{X}_u)] = 1 + z_u(\mathbf{X}_u)$ for all $u \subseteq \{1, \ldots, N\}$. Expanding the nonconstant component functions of $w(\mathbf{X})$ in terms of measure-consistent orthonormal polynomials yields

$$w_u(\mathbf{X}_u) = \sum_{\substack{\mathbf{j}_{|u|} \in \mathbb{N}_0^{|u|} \\ j_1,\ldots,j_{|u|} \neq 0}} D_{u\mathbf{j}_{|u|}}\,\psi_{u\mathbf{j}_{|u|}}(\mathbf{X}_u),\ \emptyset \neq u \subseteq \{1, \ldots, N\}, \tag{43}$$

with

$$D_{u\boldsymbol{j}_{|u|}} := \int_{\mathbb{R}^N} \ln y(\mathbf{x})\,\psi_{u\mathbf{j}_{|u|}}(\mathbf{x}_u)\, f_{\mathbf{X}}(\mathbf{x})\mathrm{d}\mathbf{x} \tag{44}$$

DOI: 10.1002/nme

defining a distinct but similar set of expansion coefficients. Finally, combining Equations (42) and (43) leads to the L-PDD of

$$y(\mathbf{X}) = \exp(w_\emptyset) \prod_{\emptyset \neq u \subseteq \{1,\ldots,N\}} \exp\left[\sum_{\substack{\mathbf{j}_{|u|} \in \mathbb{N}_0^{|u|} \\ j_1,\ldots,j_{|u|} \neq 0}} D_{u\mathbf{j}_{|u|}} \psi_{u\mathbf{j}_{|u|}}(\mathbf{X}_u) \right], \tag{45}$$

which is yet another exact representation of $y(\mathbf{X})$, where infinite orthonormal polynomials of increasing dimensions are structured with a multiplicative hierarchy, as opposed to an additive hierarchy in Equation (10). Consequently, an S-variate, mth-order L-PDD approximation, retaining at most S-variate component functions and mth-order orthogonal polynomials, becomes

$$\bar{y}_{S,m}(\mathbf{X}) = \exp(w_\emptyset) \prod_{\substack{\emptyset \neq u \subseteq \{1,\ldots,N\} \\ 1 \leqslant |u| \leqslant S}} \exp\left[\sum_{\substack{\mathbf{j}_{|u|} \in \mathbb{N}_0^{|u|}, \left\|\mathbf{j}_{|u|}\right\|_\infty \leqslant m \\ j_1,\ldots,j_{|u|} \neq 0}} D_{u\mathbf{j}_{|u|}} \psi_{u\mathbf{j}_{|u|}}(\mathbf{X}_u) \right], \tag{46}$$

which also converges to $y(\mathbf{X})$ in the mean-square sense when $S \to N$ and $m \to \infty$.

Similar to F-PDD, no simple expressions are available for the second-moment properties of $\bar{y}_{S,m}(\mathbf{X})$ when S and m are arbitrary. However, a probabilistic characteristic of $y(\mathbf{X})$ is also easily estimated by the MCS of $\bar{y}_{S,m}(\mathbf{X})$ in Equation (46). When $S = 1$, the univariate L-PDD approximation with $D_{ij} := D_{\{i\}(j)}$ becomes

$$\bar{y}_{1,m}(\mathbf{X}) = \exp(w_\emptyset) \prod_{i=1}^{N} \exp\left[\sum_{j=1}^{m} D_{ij} \psi_{ij}(X_i) \right], \tag{47}$$

forming a product of exponential functions of univariate polynomials. In which case, the approximate mean and variance of $\bar{y}_{1,m}(\boldsymbol{X})$ are readily calculated from

$$\mathbb{E}[\bar{y}_{1,m}(\mathbf{X})] = \exp(w_\emptyset) \prod_{i=1}^{N} \mathbb{E}\left[\exp\left\{ \sum_{j=1}^{m} D_{ij} \psi_{ij}(X_i) \right\} \right] \tag{48}$$

and

$$\begin{aligned} \mathbb{E}\left[(\bar{y}_{1,m}(\mathbf{X}) - \mathbb{E}[\bar{y}_{1,m}(\mathbf{X})])^2 \right] = \exp(2w_\emptyset) \prod_{i=1}^{N} \mathbb{E}\left[\exp\left\{ 2\sum_{j=1}^{m} D_{ij} \psi_{ij}(X_i) \right\} \right] \\ - \exp(w_\emptyset) \prod_{i=1}^{N} \mathbb{E}\left[\exp\left\{ \sum_{j=1}^{m} D_{ij} \psi_{ij}(X_i) \right\} \right], \end{aligned} \tag{49}$$

respectively, that are valid for an arbitrary $m < \infty$, provided that the expectations exist and are finite. It is important to note that the expectations in Equations (48) and (49) require at most univariate integrals regardless of N or m, and involve the expansion coefficients $D_{ij}, i = 1, \ldots, N$ and $j = 1, \ldots, m$, stemming from the univariate L-PDD approximation in Equation (47).

Remark 12

The A-PDD approximation $\tilde{y}_{1,m}(\mathbf{X})$ is called univariate because Equation (14) comprises a sum of at most univariate component functions, describing only the main effect of $\mathbf{X}$. In contrast, the F-PDD approximation $\hat{y}_{1,m}(\mathbf{X})$ in Equation (36) and the L-PDD approximation $\bar{y}_{1,m}(\mathbf{X})$ in Equation (47) contain products of various univariate functions. Therefore, some effects of interactions between two input variables X_i and X_j, $i \neq j$, subsist in $\hat{y}_{1,m}(\mathbf{X})$ or $\bar{y}_{1,m}(\mathbf{X})$. As an example,

DOI: 10.1002/nme

consider a function, $y = y_\emptyset + y_{\{1\}}(X_1) + y_{\{2\}}(X_2) + y_{\{1\}}(X_1)y_{\{2\}}(X_2)/y_\emptyset$, of two variables, containing a sum and a product of its univariate ANOVA component functions. The univariate A-PDD approximation, $\tilde{y}_{1,m} = y_\emptyset + y_{\{1\}}(X_1) + y_{\{2\}}(X_2)$, captures only the main effects of X_1 and X_2, and may produce nonnegligible errors if the product term of y is significant. On the other hand, the univariate F-PDD approximation $\hat{y}_{1,m} = (1 + z_\emptyset)[1 + z_{\{1\}}(X_1)][1 + z_{\{2\}}(X_2)] = y_\emptyset + y_{\{1\}}(X_1) + y_{\{2\}}(X_2) + y_{\{1\}}(X_1)y_{\{2\}}(X_2)/y_\emptyset$, obtained using the relationships in Equations (30) and (31), exactly reproduces y, thereby capturing not only the main effects but also the interactive effect of input variables. Therefore, the term 'univariate' used in this paper for the multiplicative PDD approximations should be interpreted in the context of including at most univariate component functions, not necessarily preserving only the main effects. It would be intriguing to study if a univariate approximation from a multiplicative PDD results in more accurate stochastic solutions of real-life problems than that from the additive PDD.

Remark 13

When $y_\emptyset$ is *zero* or is close to *zero*, Equations (30)–(38) may fail or become ill-conditioned, raising questions about the suitability of the F-PDD approximation in such conditions. The L-PDD approximation faces a similar situation when a stochastic response is nonpositive or close to *zero*, as the logarithmic transformation employed in Equations (39)–(49) is invalid or highly nonlinear. However, they do not necessarily imply that the L-PDD or F-PDD cannot be used. Indeed, all of these problems can be remedied by appropriately conditioning the stochastic response y. For instance, by adding a nonzero constant to y or multiplying y with a nonzero constant, Equations (30)–(38) for the preconditioned y remain valid and well behaved. Similarly, by adding a nonnegative constant to y or multiplying y with a nonzero constant, one can make the preconditioned y to always remain positive or well behaved. Section 7 describes how such problems may arise in a practical situation, including simple adjustments to work around them.

Remark 14

The MCS of PDD approximations $\tilde{y}_{S,m}(\mathbf{X})$, $\hat{y}_{S,m}(\mathbf{X})$, or $\bar{y}_{S,m}(\mathbf{X})$, referred to as embedded MCS in this paper, entails evaluations of simple analytical functions. Hence, an arbitrarily large sample size can be accommodated in an embedded MCS for estimating rare-event probabilities. In contrast, the MCS of $y(\boldsymbol{X})$, referred to as crude MCS in this paper, requires expensive numerical calculations and can, therefore, be prohibitive when estimating such probabilities.

5. EXPANSION COEFFICIENTS

The determination of the expansion coefficients $y_\emptyset$, $C_{\boldsymbol{u}\mathbf{j}_{|\boldsymbol{u}|}}$, $w_\emptyset$, and $D_{\boldsymbol{u}\mathbf{j}_{|\boldsymbol{u}|}}$ in Equations (2), (9), (40), and (44), respectively, involves various N-dimensional integrals over $\mathbb{R}^N$. For large N, a full numerical integration employing an N-dimensional tensor product of a univariate quadrature formula is computationally prohibitive. Instead, a dimension-reduction integration scheme and a sampling technique were applied to estimate the coefficients efficiently.

5.1. Dimension-reduction integration

The dimension-reduction integration, developed by Xu and Rahman [14], entails approximating a high-dimensional integral of interest by a finite sum lower-dimensional integrations. For calculating the expansion coefficients, $y_\emptyset$, $C_{\boldsymbol{u}\mathbf{j}_{|\boldsymbol{u}|}}$, $w_\emptyset$, and $D_{\boldsymbol{u}\mathbf{j}_{|\boldsymbol{u}|}}$, this is accomplished by replacing the N-variate function y or $\ln y$ in Equations (2), (9), (40), and (44) with an R-variate truncation, where $R < N$, of its referential dimensional decomposition at a chosen reference point [12, 15]. The result is a reduced integration scheme, requiring evaluations of at most R-dimensional integrals. The scheme facilitates calculation of the coefficients approaching their exact values as $R \to N$, and is significantly more efficient than performing one N-dimensional integration, particularly when $R \ll N$. Hence, the computational effort is significantly decreased using the dimension-reduction integration. When $R = 1$ or 2, the scheme involves one-dimensional or, at most, two-dimensional integrations, respectively. Nonetheless, numerical integration is still required for a general integrand.

DOI: 10.1002/nme

The integration points and associated weights, which depend on the probability distribution of X_i, are readily available when the basis functions are polynomials [2, 16]. Further details are given in Appendix A.

The S-variate, mth-order A-PDD, F-PDD, and L-PDD approximations require evaluations of $Q_{S,m} = \sum_{k=0}^{k=S} \binom{N}{S-k} m^{S-k}$ number of expansion coefficients, including $y_\emptyset$ or $w_\emptyset$. If these coefficients are estimated by dimension-reduction integration with $R = S < N$ and therefore involve at most an S-dimensional tensor product of an n-point univariate quadrature rule depending on m, then the total cost for the S-variate, mth-order approximation entails a maximum of $\sum_{k=0}^{k=S} \binom{N}{S-k} n^{S-k}(m)$ function evaluations. If the integration points include a common point in each coordinate – a special case of symmetric input probability density functions and odd values of n (see Example 3) – the number of function evaluations reduces to $\sum_{k=0}^{k=S} \binom{N}{S-k} (n(m)-1)^{S-k}$. In other words, the computational complexity of the PDD approximations is an Sth-order polynomial with respect to the number of random variables or integration points.

5.2. Sampling

Sampling techniques, including crude MCS or quasi-MCS, for estimating the expansion coefficients comprise two simple steps: (1) generate a point set $\mathcal{P}_L := \{\mathbf{x}^{(l)} \in \mathbb{R}^N,\ l = 1, \ldots, L\}$ of size $L \in \mathbb{N}$ consistent with the probability measure of the random input $\mathbf{X}$; (2) approximate the integrals in Equations (2), (9), (40), and (44) as the averages of y, $y\psi_{\mathbf{u}_{\mathbf{j}|u|}}$, $\ln y$, and $\ln y\psi_{\mathbf{u}_{\mathbf{j}|u|}}$ evaluated at all points of $\mathcal{P}_L$. In crude MCS, $\mathcal{P}_L$ contains a sequence of pseudorandom numbers, following the probability distributions of $\mathbf{X}$. In quasi-MCS, $\mathcal{P}_L$ is a set of a low-discrepancy sequence. The advantage of one MCS over the other depends on the smoothness properties of the integrand and the dimension of the integral [17].

Remark 15

It is important to emphasize that the F-PDD and L-PDD approximations involve the same or similar expansion coefficients that are defined in the additive PDD approximation. Therefore, the computational effort of the additive PDD approximation is recycled for generating both the F-PDD and L-PDD approximations. No additional computational cost is incurred by either variant of the PDD approximation.

6. NUMERICAL EXAMPLES

Three numerical examples are presented to illustrate the performance of the additive and multiplicative PDD approximations in calculating the statistical moments of random mathematical functions or random eigenvalues, including the tail probability distributions of natural frequencies. In Example 1, classical Legendre or Hermite polynomials were used to define the orthonormal polynomials, and all expansion coefficients were determined analytically. In Examples 2 and 3, all original random variables were transformed into standard Gaussian random variables, facilitating the use of Hermite orthonormal polynomials as bases and the Gauss–Hermite quadrature rule for calculating the expansion coefficients. The expansion order m varies depending on the example, but in all cases, the number of integration points $n = m + 1$. In Example 2, the sample sizes for crude MCS and the embedded MCS of all three PDD methods are 10^7. The respective sample sizes are $50,000$ and 10^6 in Example 3.

6.1. Example 1: two mathematical functions

Consider a polynomial function and an exponential function, expressed by

$$y_1(\mathbf{X}) = \frac{1}{2^N} \prod_{i=1}^{N} \left(3X_i^2 + 1\right) \text{ and} \tag{50}$$

$$y_2(\mathbf{X}) = \frac{1}{(4/5)^{N/2}} \prod_{i=1}^{N} \left[\exp\left(\frac{X_i^2}{10}\right)\right], \tag{51}$$

DOI: 10.1002/nme

respectively, where $X_i, i = 1, \ldots .N$, are independent and identical random variables. Each variable follows standard uniform distribution over [0,1] for the polynomial function and standard Gaussian distribution with *zero* mean and *unit* variance for the exponential function. From elementary calculations, the exact mean and variance of y_1 are 1 and $(6/5)^N - 1$, respectively, and those of y_2 are 1 and $(16/15)^{N/2} - 1$, respectively. The purpose of this example is to compare the second-moment statistics of both functions for $N = 5$ obtained using A-PDD (Equations (12) and (13)), F-PDD (Equations (37) and (38)), and L-PDD (Equations (48) and (49)) approximations. The integrals in Equations (48) and (49) were evaluated by $m + 1$-point Gauss–Legendre rule for y_1 but analytically for y_2.

Table I presents relative errors, defined as the ratio of the absolute difference between the exact and approximate variances of y_1 to the exact variance, committed by the additive and multiplicative PDD approximations for various combinations of the truncation parameters $1 \leqslant S \leqslant 5$ and $1 \leqslant m \leqslant 8$. The errors from A-PDD approximations drop as m increases, but they level off quickly at their respective limits for the univariate to quadrivariate A-PDD approximations. When $m = 2$, the error due to the pentavariate, second-order A-PDD approximation reaches *zero*, as the approximation coincides with y_1. The error remains *zero* for the univariate, second-order F-PDD approximation, as y_1 is a product of univariate quadratic polynomials. For the same reason, there is no need to employ higher-variate or higher-order F-PDD approximations. In contrast, the univariate L-PDD approximation also yields progressively smaller errors as m increases, but unlike in F-PDD, the error does not vanish. This is because the logarithmic transformation inducing additional nonlinearity to y_1 creates a nonpolynomial that cannot be exactly reproduced by a polynomial, regardless of how large $m < \infty$ becomes. Nonetheless, the L-PDD, which also requires only univariate approximation, is more accurate than the univariate to quadrivariate A-PDD approximations when $m \geqslant S$. Both the F-PDD and L-PDD approximations favorably exploit the multiplicative structure of y_1, but the former approximation is superior to the latter approximation when dealing with multiplicative polynomials.

Table II displays the results from similar error analysis performed for y_2, a product of univariate functions, although not polynomials. As expected, the errors emanating from A-PDD approximations decline as S or m rises. Since the pentavariate A-PDD and the univariate F-PDD of y_2 are identical polynomials, the respective errors coincide regardless of m. Again, due to a multiplicative nature of y_2, the F-PDD approximation is more appropriate to use than the A-PDD approximation. However, neither converges to exactness, as y_2 is a nonpolynomial function to begin with. In contrast, the logarithmic transformation, not beneficial to y_1, creates a polynomial image of y_2, which is, therefore, exactly reproduced by an L-PDD approximation. Indeed, the univariate, second-order L-PDD approximation yields the exact variance of y_2, turning the tables on the F-PDD

Table I. Relative errors in calculating the variance of y_1 by various polynomial dimensional decomposition approximations.

	A-PDD[a]					F-PDD[a]	L-PDD
m	$S = 1$	$S = 2$	$S = 3$	$S = 4$	$S = 5$	$S = 1$	$S = 1$
1	3.7×10^{-1}	1.3×10^{-1}	9.0×10^{-2}	8.5×10^{-2}	8.5×10^{-2}	8.5×10^{-2}	5.9×10^{-2}
2	3.3×10^{-1}	5.9×10^{-2}	5.6×10^{-3}	2.2×10^{-4}	0	0	3.7×10^{-2}
3	3.3×10^{-1}	5.9×10^{-2}	5.6×10^{-3}	2.2×10^{-4}	–[b]	–[b]	3.5×10^{-4}
4	3.3×10^{-1}	5.9×10^{-2}	5.6×10^{-3}	2.2×10^{-4}	–[b]	–[b]	8.3×10^{-7}
5	3.3×10^{-1}	5.9×10^{-2}	5.6×10^{-3}	2.2×10^{-4}	–[b]	–[b]	1.1×10^{-6}
6	3.3×10^{-1}	5.9×10^{-2}	5.6×10^{-3}	2.2×10^{-4}	–[b]	–[b]	1.6×10^{-7}
7	3.3×10^{-1}	5.9×10^{-2}	5.6×10^{-3}	2.2×10^{-4}	–[b]	–[b]	3.3×10^{-7}
8	3.3×10^{-1}	5.9×10^{-2}	5.6×10^{-3}	2.2×10^{-4}	–[b]	–[b]	3.3×10^{-7}

Note: PDD, polynomial dimensional decomposition; A-PDD, additive PDD; F-PDD, factorized PDD; L-PDD, logarithmic PDD.

[a]The variances from the pentavariate, second-order A-PDD and univariate, second-order F-PDD approximations coincide with the exact solution: $(6/5)^N - 1$, where $N = 5$.

[b]Not required.

DOI: 10.1002/nme

Table II. Relative errors in calculating the variance of y_2 by various polynomial dimensional decomposition approximations.

	A-PDD					F-PDD	L-PDD[a]
m	$S=1$	$S=2$	$S=3$	$S=4$	$S=5$	$S=1$	$S=1$
1	1	1	1	1	1	1	1
2	1.1×10^{-1}	5.2×10^{-2}	5.1×10^{-2}	5.0×10^{-2}	5.0×10^{-2}	5.0×10^{-2}	0
3	1.1×10^{-1}	5.2×10^{-2}	5.1×10^{-2}	5.0×10^{-2}	5.0×10^{-2}	5.0×10^{-2}	–[b]
4	6.6×10^{-2}	4.7×10^{-3}	2.7×10^{-3}	2.6×10^{-3}	2.6×10^{-3}	2.6×10^{-3}	–[b]
5	6.6×10^{-2}	4.7×10^{-3}	2.7×10^{-3}	2.6×10^{-3}	2.6×10^{-3}	2.6×10^{-3}	–[b]
6	6.4×10^{-2}	2.2×10^{-3}	1.8×10^{-4}	1.5×10^{-4}	1.5×10^{-4}	1.5×10^{-4}	–[b]
7	6.4×10^{-2}	2.2×10^{-3}	1.8×10^{-4}	1.5×10^{-4}	1.5×10^{-4}	1.5×10^{-4}	–[b]
8	6.4×10^{-2}	2.2×10^{-3}	5.9×10^{-5}	2.6×10^{-5}	2.6×10^{-5}	2.6×10^{-5}	–[b]

Note: PDD, polynomial dimensional decomposition; A-PDD, additive PDD; F-PDD, factorized PDD; L-PDD, logarithmic PDD.

[a] The variance from the univariate, second-order L-PDD approximation coincides with the exact solution: $(16/5)^{N/2}-1$, where $N=5$.

[b] Not required.

approximation for tackling multiplicative nonpolynomials. In summary, both functions y_1 and y_2, although simple and somewhat contrived, demonstrate a clear advantage of multiplicative PDD over additive PDD approximations.

6.2. *Example 2: eigenvalues of an undamped, spring–mass system*

Consider a two-degree-of-freedom, undamped, spring–mass system, shown in Figure 1, with random mass and random stiffness matrices

$$\boldsymbol{M}(\mathbf{X})=\begin{bmatrix} M_1(\mathbf{X}) & 0 \\ 0 & M_2(\mathbf{X}) \end{bmatrix} \text{ and } \boldsymbol{K}(\mathbf{X})=\begin{bmatrix} K_1(\mathbf{X})+K_3(\mathbf{X}) & -K_3(\mathbf{X}) \\ -K_3(\mathbf{X}) & K_2(\mathbf{X})+K_3(\mathbf{X}) \end{bmatrix}, \quad (52)$$

respectively, where $K_1(\mathbf{X}) = 1000X_1$ N/m, $K_2(\mathbf{X}) = 1100X_2$ N/m, $K_3(\mathbf{X}) = 100X_3$ N/m, $M_1(\mathbf{X}) = X_4$ kg, and $M_2(\mathbf{X}) = 1.5X_5$ kg. The input $\mathbf{X} = \{X_1, X_2, X_3, X_4, X_5\}^T \in \mathbb{R}^5$ is an independent lognormal random vector with its mean vector $\mu_{\mathbf{X}} = \mathbf{1} \in \mathbb{R}^5$ and covariance matrix $\Sigma_{\mathbf{X}} = \text{diag}\left(v_1^2, v_2^2, v_3^2, v_4^2, v_5^2\right) \in \mathbb{R}^{5\times5}$, where v_i, $i = 1,\ldots,5$, representing the coefficients of variation of X_i, are as follows: $v_1 = v_2 = 0.25$, $v_3 = v_4 = v_5 = 0.125$. There exist two real-valued random eigenvalues, $\lambda_1(\mathbf{X})$ and $\lambda_2(\mathbf{X})$, which are sorted into an ascending order.

Since the eigenvalues are in general nonpolynomial functions of input, a convergence study with respect to the truncation parameters of PDD approximations is required to calculate the probabilistic characteristics of eigensolutions accurately. The expansion coefficients were calculated by a full five-dimensional tensor product of an $m+1$-point, univariate Gauss–Hermite quadrature formula. Figure 2(a) and Figure 2(b) depict how the relative errors in the probabilities, $P[\lambda_1(\mathbf{X}) \leqslant \lambda_{01}]$ and $P[\lambda_2(\mathbf{X}) \leqslant \lambda_{02}]$, of the two random eigenvalues decay with respect to S for $m = 15$ when the thresholds $\lambda_{01} = 780$ (rad/s)^2; $\lambda_{02} = 1200$ (rad/s)^2 and $\lambda_{01} = 300$ (rad/s)^2; $\lambda_{02} = 565$ (rad/s)^2, respectively. The relative error is defined as the ratio of the absolute difference in the probabilities estimated by crude MCS and embedded MCS of PDD approximations to the probability calculated by crude MCS. When $\lambda_{01} = 780$ (rad/s)^2; $\lambda_{02} = 1200$ (rad/s)^2, the probabilities are relatively large,

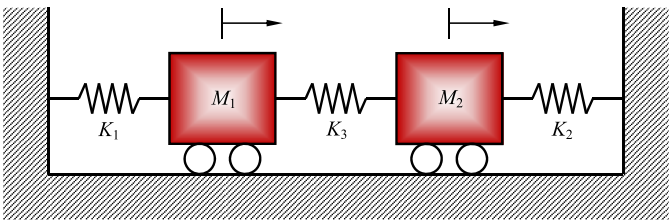

Figure 1. A two-degree-of-freedom, undamped, spring–mass system.

DOI: 10.1002/nme

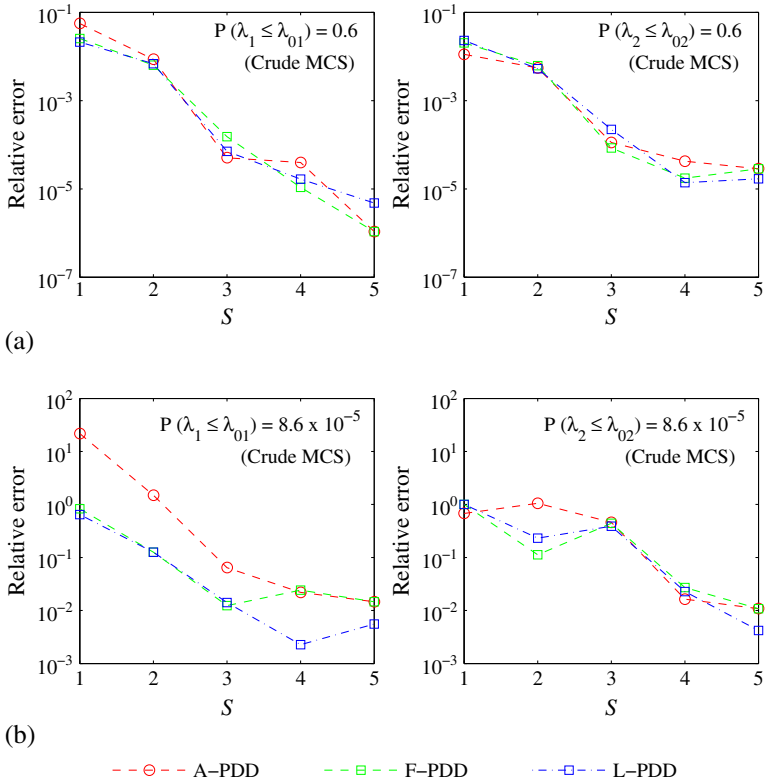

Figure 2. Relative errors in $P[\lambda_1(\mathbf{X}) \leqslant \lambda_{01}]$, $P[\lambda_2(\mathbf{X}) \leqslant \lambda_{02}]$ of the spring–mass system by various polynomial dimensional decomposition (PDD) methods: (a) $\lambda_{01} = 780$ (rad/s)^2, $\lambda_{02} = 1200$ (rad/s)^2; (b) $\lambda_{01} = 300$ (rad/s)^2, $\lambda_{02} = 565$ (rad/s)^2. Note: MCS, Monte Carlo simulation; A-PDD, additive PDD; F-PDD, factorized PDD; L-PDD, logarithmic PDD.

for which, according to Figure 2(a), there is no notable difference in the errors from the A-PDD, F-PDD, and L-PDD approximations. Therefore, any of the three approximations can be a method of choice. However, when $\lambda_{01} = 300$ (rad/s)^2; $\lambda_{02} = 565$ (rad/s)^2, the probabilities are relatively small, in which case the lower-variate ($S = 1$ or 2) F-PDD and L-PDD approximations, shown in Figure 2(b), commit smaller errors than the corresponding A-PDD approximations do. Therefore, a multiplicative PDD approximation may be preferred over an additive PDD approximation when calculating the tail distributions of a stochastic response.

6.3. Example 3: modal analysis of a functionally graded cantilever plate

The third example involves free vibration analysis of a $2\,\mathrm{m} \times 1\,\mathrm{m} \times 10\,\mathrm{mm}$ cantilever plate, shown in Figure 3(a), made of a functionally graded material (FGM)[§], where silicon carbide (SiC) particles varying along the horizontal coordinate ξ are randomly dispersed in an aluminum (Al) matrix. The result is a random inhomogeneous plate, where the effective elastic modulus $E(\xi)$, effective Poisson's ratio $\nu(\xi)$, and effective mass density $\rho(\xi)$ are random fields. They depend on two principal sources of uncertainties: (1) randomness in the volume fraction of SiC particles $\phi_{\mathrm{SiC}}(\xi)$, which varies only along ξ, and (2) randomness in constituent material properties, comprising elastic moduli E_{SiC} and E_{Al}, Poisson's ratios ν_{SiC} and ν_{Al}, and mass densities ρ_{SiC} and ρ_{Al} of SiC and Al material phases, respectively. The particle volume fraction $\phi_{\mathrm{SiC}}(\xi)$ is a one-dimensional, inhomogeneous, Beta random field with mean $\mu_{\mathrm{SiC}}(\xi) = 1-\xi/L$ and standard deviation $\sigma_{\mathrm{SiC}}(\xi) = (\xi/L)(1-\xi/L)$, where L is the length of the plate. Assuming an appropriately bounded covariance function of

[§]Functionally graded materials are two-phase or multiphase particulate composites in which material composition and microstructure vary spatially in the macroscopic length scale to meet a desired functional performance.

DOI: 10.1002/nme

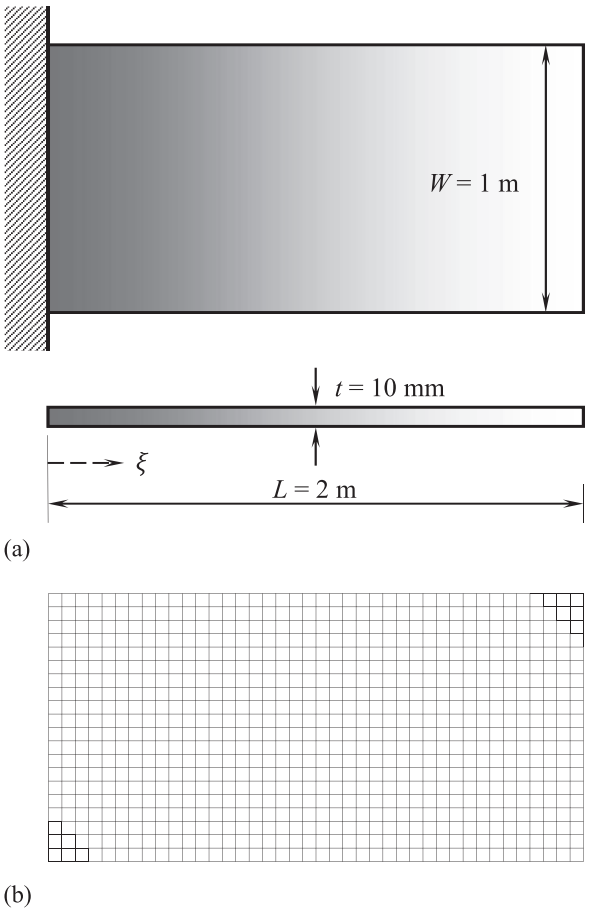

Figure 3. A functionally graded material cantilever plate: (a) geometry; (b) a 20 × 40 finite-element analysis mesh.

Table III. Statistical material properties of constituents in SiC–Al functionally graded material.

Material properties[a]	Mean	Coefficient of variation, %
E_{SiC}, GPa	419.2	15
ν_{SiC}	0.19	5
ρ_{SiC}, kg/m^3	3210	15
E_{Al}, GPa	69.7	15
ν_{Al}	0.34	5
ρ_{Al}, kg/m^3	2520	15

[a] E_{SiC} = elastic modulus of SiC, ν_{SiC} = Poisson's ratio of SiC, ρ_{SiC} = mass density of SiC, E_{Al} = elastic modulus of Al, ν_{Al} = Poisson's ratio of Al, ρ_{Al} = mass density of Al.

$\phi_{\mathrm{SiC}}(\xi)$, the standardized volume fraction $\tilde{\phi}_{\mathrm{SiC}}(\xi) := [\phi_{\mathrm{SiC}}(\xi) - \mu_{\mathrm{SiC}}(\xi)]/\sigma_{\mathrm{SiC}}(\xi)$ was mapped to a zero-mean, homogeneous, Gaussian image field $\alpha(\xi)$ with an exponential covariance function $\Gamma_\alpha(t) := \mathbb{E}[\alpha(\xi)\alpha(\xi + t)] = \exp(-|t|/0.125L)$ via $\tilde{\phi}_{\mathrm{SiC}}(\xi) = F^{-1}_{\mathrm{SiC}}[\Phi(\alpha(\xi))]$, where Φ is the distribution function of a standard Gaussian random variable and F_{SiC} is the marginal distribution function of $\tilde{\phi}_{\mathrm{SiC}}(\xi)$. The Karhunen–Loève approximation [18] was employed to discretize $\alpha(\xi)$ and hence $\phi_{\mathrm{SiC}}(\xi)$ into 28 standard Gaussian random variables. In addition, the constituent material properties, E_{SiC}, E_{Al}, ν_{SiC}, ν_{Al}, ρ_{SiC}, and ρ_{Al}, were modeled as independent lognormal random variables with their means and coefficients of variation described in Table III.

DOI: 10.1002/nme

Therefore, a total of 34 random variables are involved in this example. Employing a rule of mixture, $E(\xi) \cong E_{\mathrm{SiC}}\phi_{\mathrm{SiC}}(\xi) + E_{\mathrm{Al}}[1-\phi_{\mathrm{SiC}}(\xi)]$, $\nu(\xi) \cong \nu_{\mathrm{SiC}}\phi_{\mathrm{SiC}}(\xi) + \nu_{\mathrm{Al}}[1-\phi_{\mathrm{SiC}}(\xi)]$, and $\rho(\xi) \cong \rho_{\mathrm{SiC}}\phi_{\mathrm{SiC}}(\xi) + \rho_{\mathrm{Al}}[1-\phi_{\mathrm{SiC}}(\xi)]$. Using these spatially-variant effective properties, a 20×40 mesh consisting of 800 eight-noded, second-order shell elements, shown in Figure 3(b), was constructed for finite-element analysis (FEA) to determine the natural frequencies of the FGM plate. No damping was included. A Lanczos algorithm [19] was employed for calculating the eigenvalues.

The probability distributions of natural frequencies of the FGM plate were evaluated using the univariate, fourth-order A-PDD, F-PDD, and L-PDD approximations, including crude MCS. The expansion coefficients of the PDD approximations were estimated using dimension-reduction integration with $R = S = 1$ and $n = 5$. Figure 4 presents the marginal probability distributions $F_i(\omega_i) := P[\Omega_i \leqslant \omega_i]$ of the first six natural frequencies Ω_i, $i = 1, \ldots, 6$, where the PDD solutions were obtained from embedded MCS. The plots are made over a semilogarithmic scale to delineate the distributions in the tail regions. For all six frequencies, the probability distributions obtained from the F-PDD and L-PDD approximations are much closer to the crude Monte Carlo results compared with those obtained from the A-PDD approximation. Each PDD approximation requires only 137 FEA, which is significantly lower than the 50,000 FEA employed by crude MCS, to generate the small probabilities in Figure 4.

Figure 5 displays the joint probability density function $f_{12}(\omega_1, \omega_2)$ of the first two natural frequencies Ω_1 and Ω_2 obtained by crude MCS and the univariate, fourth-order A-PDD, L-PDD, and

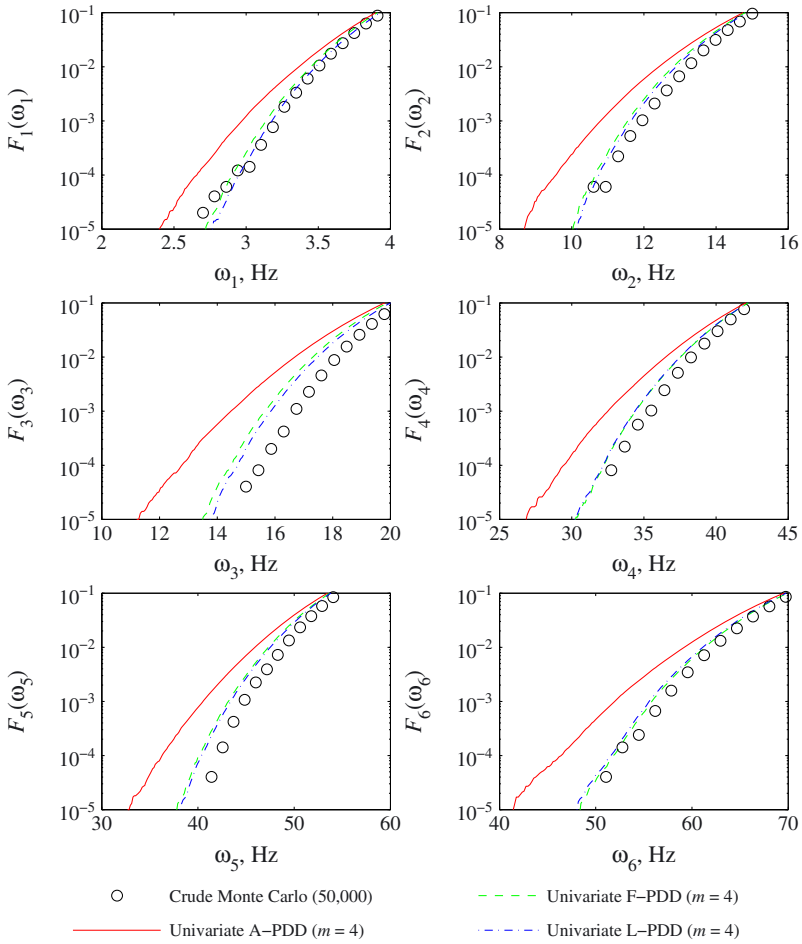

Figure 4. Marginal probability distributions of the first six natural frequencies of the functionally graded material plate by various polynomial dimensional decomposition (PDD) approximations and crude Monte Carlo simulation. Note: A-PDD, additive PDD; F-PDD, factorized PDD; L-PDD, logarithmic PDD.

DOI: 10.1002/nme

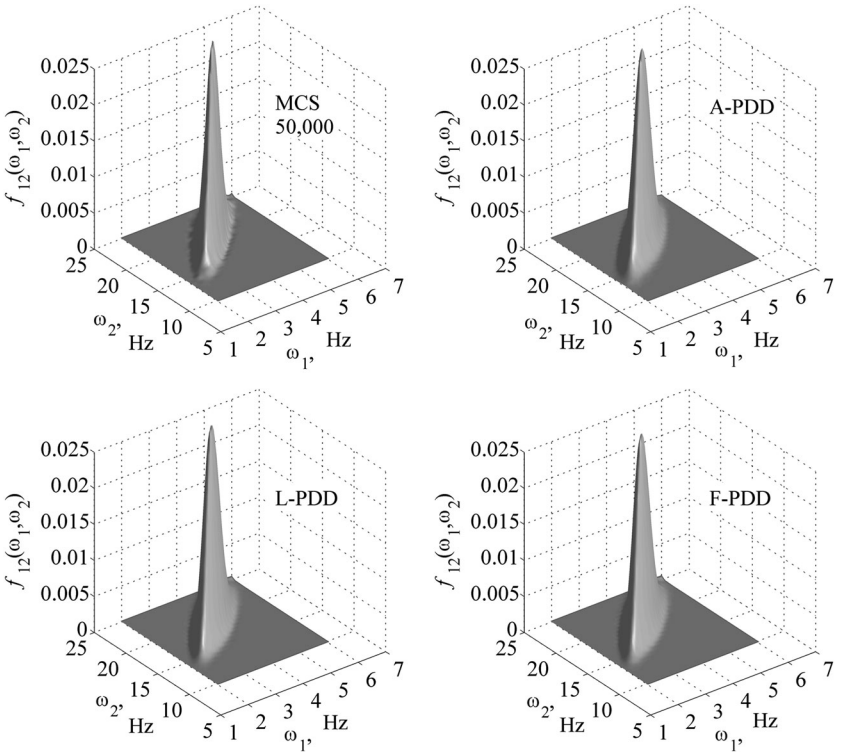

Figure 5. Joint probability density function of the first and second natural frequencies of the functionally graded material plate by various polynomial dimensional decomposition (PDD) approximations and crude Monte Carlo simulation (MCS). Note: A-PDD, additive PDD; F-PDD, factorized PDD; L-PDD, logarithmic PDD.

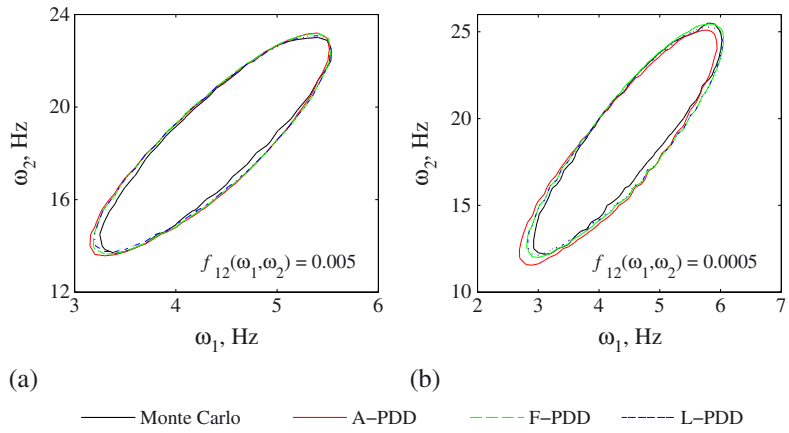

Figure 6. Contours of the joint density function of the first and second natural frequencies of the functionally graded material plate by various polynomial dimensional decomposition (PDD) approximations and crude Monte Carlo simulation: (a) $f_{12} = 0.005$; (b) $f_{12} = 0.0005$. Note: A-PDD, additive PDD; F-PDD, factorized PDD; L-PDD, logarithmic PDD.

F-PDD approximations. Although visually comparing these three-dimensional plots is not simple, the joint distributions from all three PDD approximations and the crude Monte Carlo method seem to match reasonably well. Indeed, the contours evaluated at a relatively high level, for instance $f_{12} = 0.005$, and exhibited in Figure 6(a) confirm a fairly good agreement among all four distributions. However, when examined at a relatively low level, for instance $f_{12} = 0.0005$, the contours in

DOI: 10.1002/nme

Figure 6(b) reveal the F-PDD or L-PDD approximation to be more accurate than the A-PDD approximation. These findings are consistent with the marginal distributions of natural frequencies discussed in the preceding paragraph. It appears that a lower-variate multiplicative PDD approximation, in this case a univariate F-PDD or L-PDD approximation, may provide more accurate probabilistic characteristics of a stochastic response than a univariate additive PDD approximation. This is because a univariate multiplicative PDD approximation subsumes some interactive effects of input variables, as alluded to in Remark 12.

7. APPLICATION

This section illustrates the effectiveness of the proposed multiplicative PDD methods in solving a large-scale practical engineering problem. The application involves predicting the dynamic behavior of a sport utility vehicle (SUV) in terms of the statistical properties of mode shapes and frequency response functions.

7.1. A sport utility vehicle body-in-white model

Figure 7(a) presents a computer-aided design model of an SUV body-in-white (BIW), referring to the automotive design stage where a car body's sheet metal components have been welded together, before moving parts, motor, chassis subassemblies, and trim have been added. The BIW consists of the bare metal shell of the frame body, including fixed windshields. A finite-element mesh of the model, comprising 127,213 linear shell elements and 794,292 active degrees of freedom, is displayed in Figure 7(b). Portrayed in Figure 7(a), the computer-aided design model contains 17 distinct materials having random properties, including 17 Young's moduli and 17 mass densities. In addition, six of these materials, which are used in ceiling, floor, hood, and side body of the vehicle, have random structural damping factors. In aggregate, there exist 40 random variables X_i, $i = 1, \ldots, 40$, as follows: X_1 to X_{17} = Young's moduli of materials 1 to 17; X_{18} to X_{34} = mass densities of materials 1 to 17; and X_{35} to X_{40} = damping factors of materials 1 to 6. Their means, $\mu_i := \mathbb{E}[X_i]$, $i = 1, \ldots, 40$, are listed in Table IV. Each variable follows an independent, truncated Gaussian distribution with lower limit $a_i = 0.55\mu_i$, upper limit $b_i = 1.45\mu_i$, and coefficient of variation $v_i = 0.15$. The deterministic Poisson's ratios are as follows: 0.28 for materials 1 to 13; 0.2 for materials 14 and 15; and 0.3 for materials 16 and 17.

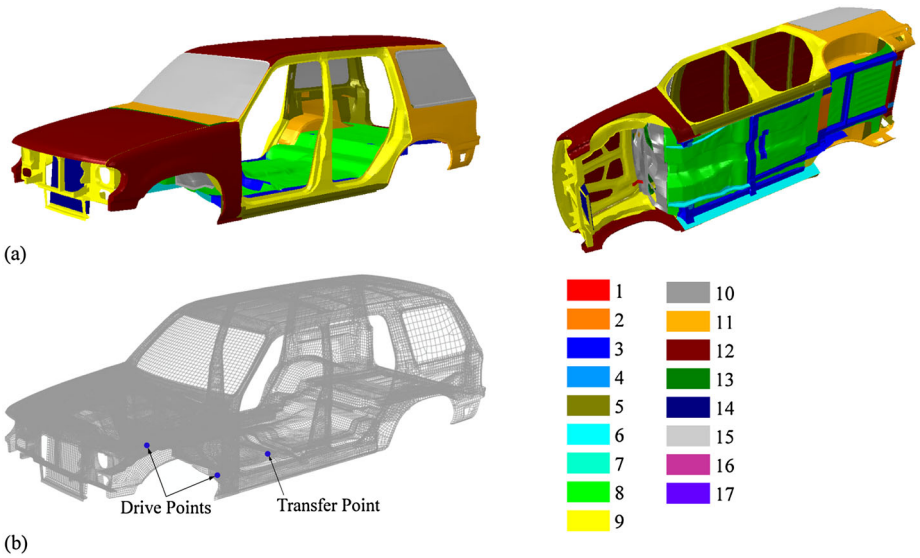

Figure 7. A sport utility vehicle body-in-white: (a) a computer-aided design model; (b) a finite-element analysis mesh.

DOI: 10.1002/nme

Table IV. Mean values of the random input variables for a sport utility vehicle body-in-white.

Material	Young's modulus, GPa	Mass density, kg/m^3	Structural damping factor, %[a]
1	207	9500	1
2	207	9500	1
3	207	8100	1
4	207	29,260	1
5	207	29,260	1
6	207	37,120	1
7	207	9500	–[b]
8	207	8100	–[b]
9	207	8100	–[b]
10	207	29,260	–[b]
11	207	30,930	–[b]
12	207	37,120	–[b]
13	207	52,010	–[b]
14	69	2700	–[b]
15	69	2700	–[b]
16	20	1189	–[b]
17	200	1189	–[b]

[a]Structural damping, best suited for frequency domain analysis, assumes that the damping forces are proportional to the forces caused by stressing of the structure and are opposed to the velocity.
[b]The damping factors for materials 7–17 are equal to zero (deterministic).

7.2. *Steady-state dynamic analysis*

A mode-based steady-state dynamic analysis consists of two steps: an eigensolution extraction, followed by a frequency response calculation. For obtaining eigensolutions, the upper bound of the frequency extraction range was chosen as 300 Hz, and the frequency response functions were computed up to 150 Hz. The automatic multilevel substructuring method [20] embedded in ABAQUS (Version 6.11) [21] was employed for extracting natural frequencies and mode shapes. The automatic multilevel substructuring eigensolver approximates global eigenmodes below the global cutoff frequency of 300 Hz, and the frequency response solutions below 150 Hz were calculated at 1 Hz increments. Since the BIW model is not constrained, there exist six rigid body modes.

For the steady-state dynamic analysis, the rolling motion of the vehicle was simulated by applying two harmonic loads with concentrated vertical force of unit amplitude at the nodes, called drive points, located at the two pivot points on the bottom of the vehicle floor. The frequency response functions were calculated at a node, called the transfer point, under the driver's seat. The drive and transfer points are marked in Figure 7(b).

Due to the uncertainty in material properties, the eigensolutions or frequency response functions are stochastic. The univariate, second-order multiplicative PDD approximations were employed to find their second-moment characteristics and various response probabilities. The associated expansion coefficients of PDD were estimated by crude MCS with 500 samples. The sample size for the embedded MCS of the PDD approximations varies from 10^4 to 10^6, depending on the response desired.

7.3. *Results*

7.3.1. Moments of mode shapes. The univariate, second-order F-PDD and L-PDD approximations were employed to calculate the second-moment statistics of each nodal displacement component of an eigenvector describing the associated mode shape of the BIW structure. All input random variables were transformed into standard Gaussian random variables, permitting the use of Hermite orthonormal polynomials as basis functions. For F-PDD, the statistics were calculated

DOI: 10.1002/nme

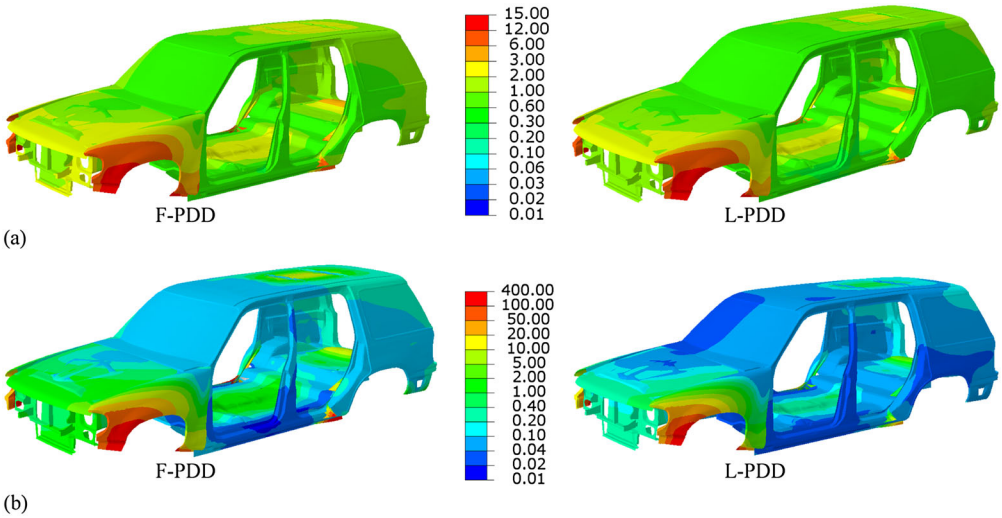

Figure 8. Contour plots of the $\mathcal{L}_2$-norm of the 21st mode shape of a sport utility vehicle body-in-white by two multiplicative polynomial dimensional decomposition (PDD) approximations: (a) mean; (b) variance. Note: F-PDD, factorized PDD; L-PDD, logarithmic PDD.

directly using Equations (37) and (38). However, for L-PDD, the statistics were estimated from the embedded MCS of Equation (47), sidestepping the need to evaluate the integrals in Equations (48) and (49) for each displacement component at all nodes. When a displacement y is nonpositive, the mean plus ten times the standard deviation of y, estimated from crude MCS used in obtaining the coefficients, was added, resulting in a positive displacement required by L-PDD. No conditioning was needed or performed for F-PDD. These simple modifications aid in calculating the means and variances of displacement components at all nodes. Based on these statistics, the $\mathcal{L}_2$-norms (square root of sum of squares) of the mean and variance of a nodal displacement were calculated. Figure 8(a) and Figure 8(b) present contour plots of the $\mathcal{L}_2$-norms of the means and variances, respectively, of an arbitrarily selected 21st mode shape, calculated using the F-PDD and L-PDD approximations. Both approximations yield reasonably close statistical moments, including the variances of the mode shape. Similar results can be generated for other mode shapes if desired.

7.3.2. Percentile functions of receptance, mobility, and inertance. For mode-based steady-state dynamic analysis, three types of frequency response functions were examined: receptance, mobility, and inertance. They are approximated by

$$u_{p,d_1d_2t}(\omega) \simeq (i\omega)^p \sum_{k=1}^{K} \frac{\left[\phi_{k,d_1} + \phi_{k,d_2}\right]\phi_{k,t}}{\left[\Omega_k^2(1+is_k) - \omega^2\right]} \tag{53}$$

where $i = \sqrt{-1}$, K is the number of eigenmodes retained, ϕ_{k,d_1} and ϕ_{k,d_2} are the two drive point vertical components of the kth eigenmode, $\phi_{k,t}$ is the transfer point vertical component of the kth eigenmode, Ω_k is the kth eigenfrequency, s_k is its corresponding structural damping factor, and ω is the excitation frequency over which the frequency response function is desired. The exponent p corresponds to the type of frequency response calculated: $p = 0$ for receptance, $p = 1$ for mobility, and $p = 2$ for inertance. All three frequency response functions are commonly used in the automotive industry to evaluate the dynamic performance of vehicle designs. For random input, it is insightful to study the probabilities of receptance and mobility for a vehicle subjected to a range of excitation frequency. When a frequency response function y is positive, but very close to zero, it was multiplied by a factor of $10^{-\log y}$, creating a well-behaved function in L-PDD. No such conditioning was required in F-PDD. Figure 9(a–c) shows various percentiles of real parts of receptance, mobility, and inertance under the driver's seat, respectively, obtained from the two univariate multiplicative

DOI: 10.1002/nme

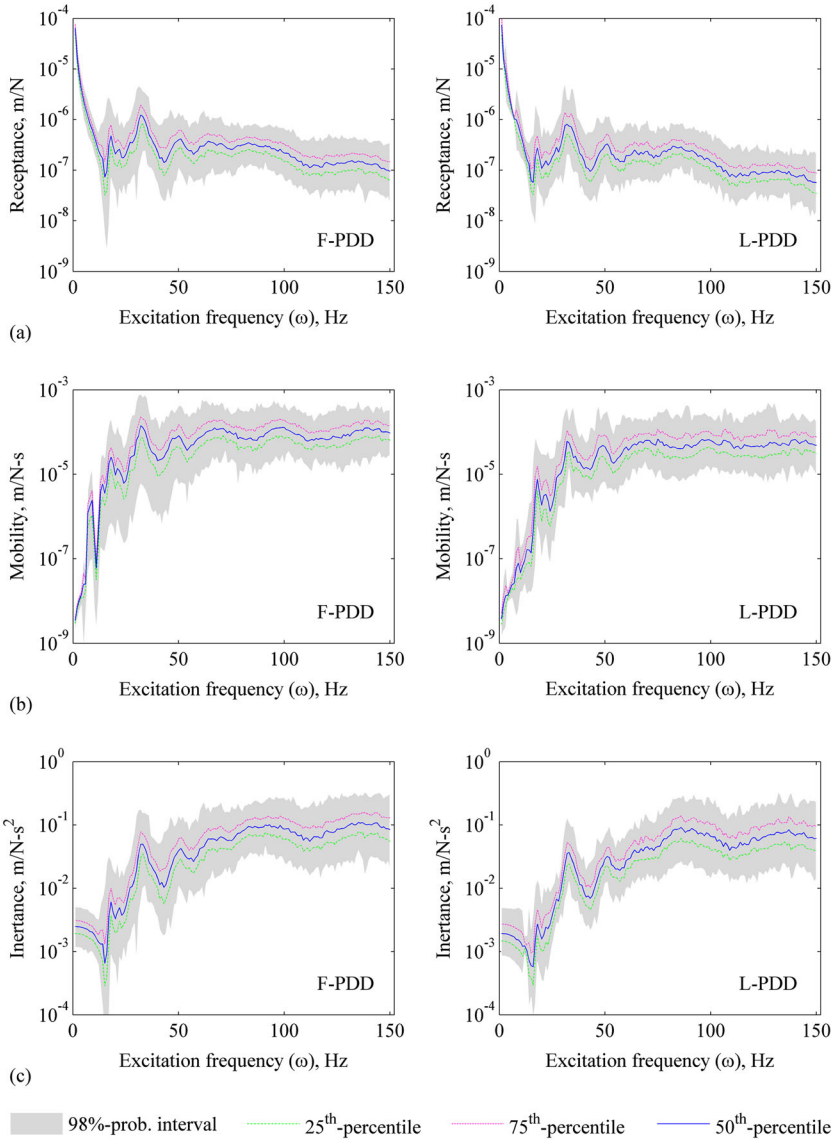

Figure 9. Percentiles of real parts of frequency response functions at the driver's seat of a sport utility vehicle body-in-white by two multiplicative polynomial dimensional decomposition (PDD) approximations: (a) receptance; (b) mobility; (c) inertance. Note: F-PDD, factorized PDD; L-PDD, logarithmic PDD.

PDD approximations. The respective results for imaginary parts are depicted in Figure 10(a–c). In both sets of figures, the percentiles were calculated from 10^4 embedded MCS of each PDD approximation at an increment of 1 Hz for the excitation frequency range of 1 to 150 Hz. Again, both the F-PDD and L-PDD approximations produce similar results. Therefore, either of the multiplicative PDD methods can be used for stochastic dynamic analysis.

7.3.3. Acceleration probabilities. Finally, Table V presents the probabilities of a weighted root mean square value of the vertical component of the acceleration under the driver's seat lying within the following intervals: $[0, 0.315]$ (not uncomfortable), $[0.315, 0.63]$ (a little uncomfortable), $[0.5, 1]$ (fairly uncomfortable), $[0.8, 1.6]$ (uncomfortable), $[1.25, 2.5]$ (very uncomfortable), and $[2, \infty)$ (extremely uncomfortable). These intervals, developed and calibrated by the International Standard ISO 2631 [22], define acceptable values of accelerations inside a vehicle for various levels of passenger comfort. The higher the interval endpoints, the harsher the level of passenger

DOI: 10.1002/nme

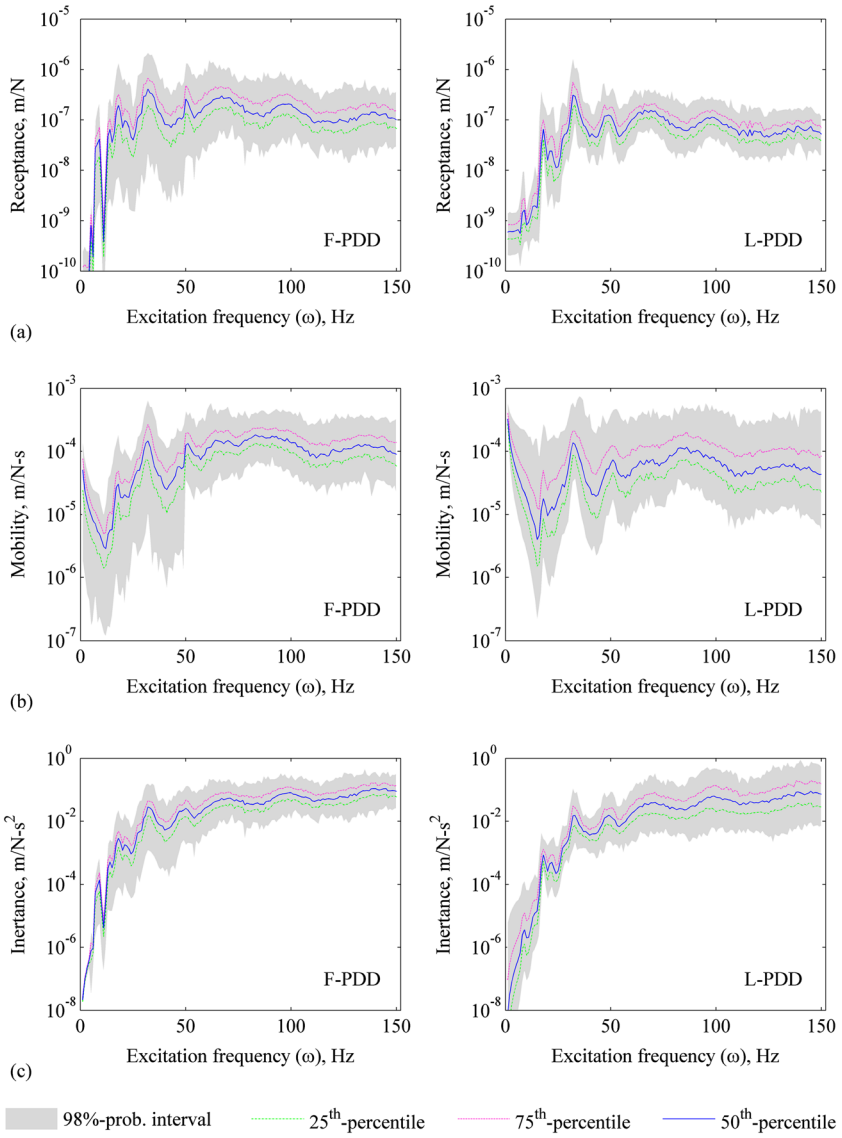

Figure 10. Percentiles of imaginary parts of frequency response functions at the driver's seat of a sport utility vehicle body-in-white by two multiplicative polynomial dimensional decomposition (PDD) approximations: (a) receptance; (b) mobility; (c) inertance. Note: F-PDD, factorized PDD; L-PDD, logarithmic PDD.

Table V. Probabilities of acceleration under the driver's seat of a sport utility vehicle body-in-white.

	Interval of acceptable accelerations, m/s^{2}[a]					
Method	$[0, 0.315]$	$[0.315, 0.63]$	$[0.5, 1]$	$[0.8, 1.6]$	$[1.25, 2.5]$	$[2, \infty)$
A-PDD	7.4×10^{-1}	2.6×10^{-1}	3.1×10^{-3}	0	0	0
F-PDD	6.9×10^{-1}	2.7×10^{-1}	3.6×10^{-2}	3.2×10^{-3}	7.3×10^{-4}	4.1×10^{-4}
L-PDD	8.4×10^{-1}	1.1×10^{-1}	3.4×10^{-2}	8.8×10^{-3}	2.1×10^{-3}	4.3×10^{-4}

Note: PDD, polynomial dimensional decomposition; A-PDD, additive PDD; F-PDD, factorized PDD; L-PDD, logarithmic PDD.

[a]From International Standard ISO 2631 [22].

experience. The weighted root mean square acceleration, obtained for an assumed applied load of 1000 N, was calculated from $\left[(1/150)\sum_{j=1}^{150}\{1000\alpha_j u_{2,d_1 d_2 t}(\omega_j)\}^2\right]^{1/2}$, where α_j and ω_j are the j th weight and excitation frequency, respectively [22].

DOI: 10.1002/nme

The probabilities were calculated by the univariate, second-order A-PDD, F-PDD, and L-PDD approximations and 10^6 embedded MCS. The acceleration probabilities in Table V predicted by both versions of the multiplicative PDD approximations have the same order and are reasonably close to each other, considering their low values. In contrast, the additive PDD approximation either significantly underpredicts or fails altogether in calculating the probabilities for all intervals examined. Therefore, the multiplicative PDD methods afford stochastic solutions that are unattainable by the additive PDD method, at least, in this problem.

It is important to emphasize that the probabilistic characteristics of eigensolutions or frequency response functions reported here were generated using only 500 FEA, representing the computational effort by the multiplicative PDD methods. Obtaining percentile functions or acceleration probabilities employing 10^4 or 10^6 crude MCS would be computationally prohibitive in today's desktop computing environment, illustrating the efficacy of the PDD methods. Furthermore, the methods developed are nonintrusive and can be easily adapted to solving complex stochastic problems requiring external legacy codes.

8. CONCLUSIONS

Two new multiplicative variants of PDD, namely factorized PDD and logarithmic PDD, were developed for uncertainty quantification of high-dimensional complex systems. They are based on hierarchical, multiplicative decompositions of a multivariate function in terms of lower-variate component functions, Fourier-polynomial expansions of lower-variate component functions by measure-consistent orthonormal polynomial bases, and a dimension-reduction integration or sampling technique for estimating the expansion coefficients. Compared with the existing, additive PDD, the factorized and logarithmic PDDs exploit the multiplicative dimensional hierarchy of a stochastic response when it exists. Since both PDDs are rooted in the ANOVA dimensional decomposition, their existence and uniqueness are guaranteed for a square-integrable function. A theorem, proven herein, reveals the relationship between all component functions of factorized PDD and ANOVA dimensional decomposition, so far available only for the univariate and bivariate component functions. Similar to the additive PDD, truncations of a multiplicative PDD lead to a convergent sequence of lower-dimensional estimates of the probabilistic characteristics of a general stochastic response. Using the properties of orthogonal polynomials, explicit formulae were derived for calculating the response statistics by the univariate factorized PDD and univariate logarithmic PDD approximations in terms of the expansion coefficients. Unlike the univariate additive PDD approximation, which captures only the main effects of input variables, a univariate truncation of multiplicative PDD includes some effects of interactions among input variables.

The additive and multiplicative PDD methods were employed to calculate the second-moment properties and tail probability distributions in three numerical problems, where the output functions are either simple mathematical functions or eigenvalues of dynamic systems, including natural frequencies of an FGM plate. When a function is purely multiplicative, the factorized or logarithmic PDD requires at most univariate approximation, resulting in a much faster convergence than the additive PDD approximation. However, the relative superiority of one multiplicative PDD approximation over the other depends on the nature of the function and whether a logarithmic transformation enhances or reduces the nonlinearity of the function. A similar trend was observed when calculating small probabilities of eigenvalues of a linear oscillator, where the multiplicative PDDs commit lower errors than does the additive PDD at lower-variate approximations. Given the same computational effort of univariate approximations, both variants of the multiplicative PDD yield more accurate tail probabilistic characteristics of natural frequencies of an FGM plate than the additive PDD. Finally, a successful evaluation of random eigensolutions of a SUV represents a significant advance in the ability of the new methods in solving practical engineering problems.

Neither variant of the multiplicative PDD approximation encounters additional cost to that required by the additive PDD approximation. Indeed, the computational complexities of all three variants of the PDD approximation are identical and polynomial, as opposed to exponential, with respect to the number of input variables. Therefore, a PDD approximation, whether additive or multiplicative, mitigates the curse of dimensionality to some degree.

DOI: 10.1002/nme

APPENDIX A: DIMENSION-REDUCTION INTEGRATION OF COEFFICIENTS

Let $\mathbf{c} = (c_1, \ldots, c_N) \in \mathbb{R}^N$ be a reference point of $\mathbf{X}$ and $y(\mathbf{x}_v, \mathbf{c}_{-v})$ represent an $|v|$-variate component function of $y(\mathbf{x})$, $v \subseteq \{1, \ldots, N\}$. Replacing $y(\mathbf{x})$ with an R-variate truncation of its referential dimensional decomposition [12, 15], the coefficients $y_\emptyset$, $C_{u\mathbf{j}_{|u|}}$, $w_\emptyset$, and $D_{u\mathbf{j}_{|u|}}$ are estimated from [14]

$$y_\emptyset \cong \sum_{k=0}^{R} (-1)^k \binom{N-R+k-1}{k} \sum_{\substack{v \subseteq \{1,\ldots,N\} \\ |v|=R-k}} \int_{\mathbb{R}^{|v|}} y(\mathbf{x}_v, \mathbf{c}_{-v}) f_{\mathbf{X}_v}(\mathbf{x}_v) \mathrm{d}\mathbf{x}_v, \tag{A.1}$$

$$C_{u\mathbf{j}_{|u|}} \cong \sum_{k=0}^{R} (-1)^k \binom{N-R+k-1}{k} \sum_{\substack{v \subseteq \{1,\ldots,N\} \\ |v|=R-k, u \subseteq v}} \int_{\mathbb{R}^{|v|}} y(\mathbf{x}_v, \mathbf{c}_{-v}) \psi_{u\mathbf{j}_{|u|}}(\mathbf{x}_u) f_{\mathbf{X}_v}(\mathbf{x}_v) \mathrm{d}\mathbf{x}_v, \tag{A.2}$$

$$w_\emptyset \cong \sum_{k=0}^{R} (-1)^k \binom{N-R+k-1}{k} \sum_{\substack{v \subseteq \{1,\ldots,N\} \\ |v|=R-k}} \int_{\mathbb{R}^{|v|}} \ln y(\mathbf{x}_v, \mathbf{c}_{-v}) f_{\mathbf{X}_v}(\mathbf{x}_v) \mathrm{d}\mathbf{x}_v, \tag{A.3}$$

$$D_{u\mathbf{j}_{|u|}} \cong \sum_{k=0}^{R} (-1)^k \binom{N-R+k-1}{k} \sum_{\substack{v \subseteq \{1,\ldots,N\} \\ |v|=R-k, u \subseteq v}} \int_{\mathbb{R}^{|v|}} \ln y(\mathbf{x}_v, \mathbf{c}_{-v}) \psi_{u\mathbf{j}_{|u|}}(\mathbf{x}_u) f_{\mathbf{X}_v}(\mathbf{x}_v) \mathrm{d}\mathbf{x}_v, \tag{A.4}$$

respectively, requiring evaluation of at most R-dimensional integrals.

ACKNOWLEDGEMENT

The authors would like to acknowledge financial support from the U.S. National Science Foundation under Grant Nos. CMMI-0653279 and CMMI-1130147.

REFERENCES

1. Rahman S. A polynomial dimensional decomposition for stochastic computing. *International Journal for Numerical Methods in Engineering* 2008; **76**:2091–2116.
2. Rahman S. Extended polynomial dimensional decomposition for arbitrary probability distributions. *Journal of Engineering Mechanics* 2009; **135**(12):1439–1451.
3. Rahman S. Statistical moments of polynomial dimensional decomposition. *Journal of Engineering Mechanics* 2010; **136**(7):923–927.
4. Bellman R. *Dynamic Programming*. Princeton University Press: Princeton, NJ, 1957.
5. Rahman S, Yadav V. Orthogonal polynomial expansions for solving random eigenvalue problems. *International Journal for Uncertainty Quantification* 2011; **1**:163–187.
6. Sobol IM. Multidimensional quadrature formulas and haar functions. *Nauka, Moscow* 1969. In Russian.
7. Sobol IM. Theorems and examples on high dimensional model representation. *Reliability Engineering & System Safety* 2003; **79**(2):187 –193.
8. Efron B, Stein C. The jackknife estimate of variance. *The Annals of Statistics* 1981; **9**(3):586–596.
9. Owen AB. Monte Carlo variance of scrambled net quadrature. *SIAM Journal on Numerical Analysis* 1997; **34**(5):1884–1910.
10. Rabitz H, Alis O. General foundations of high dimensional model representations. *Journal of Mathematical Chemistry* 1999; **25**:197–233. DOI: 10.1023/A:1019188517934.
11. Kuo FY, Sloan IH, Wasilkowski GW, Wozniakowski H. On decompositions of multivariate functions. *Mathematics of Computation* 2011; **79**:953–966.
12. Rahman S. Approximation errors in truncated dimensional decompositions, 2011. Submitted to Mathematics of Computation.
13. Tunga MA, Demiralp M. A factorized high dimensional model representation on the nodes of a finite hyperprismatic regular grid. *Applied Mathematics and Computation* 2005; **164**:865–883.

14. Xu H, Rahman S. A generalized dimension-reduction method for multi-dimensional integration in stochastic mechanics. *International Journal for Numerical Methods in Engineering* 2004; **61**:1992–2019.
15. Xu H, Rahman S. Decomposition methods for structural reliability analysis. *Probabilistic Engineering Mechanics* 2005; **20**(3):239 –250.
16. Gautschi W. *Orthogonal Polynomials: Computation and Approximation*, Numerical Mathematics and Scientific Computation. Oxford University Press: London, UK, 2004.
17. Morokoff WJ, Caflisch RE. Quasi-Monte Carlo integration. *Journal of Computational Physics* 1995; **122**:218–230.
18. Davenport WB, Root WL. *An Introduction to the Theory of Random Signals and Noise*. McGraw-Hill: New York, NY, 1958.
19. Cullum JK, Willoughby RA. *Lanczos Algorithms for Large Symmetric Eigenvalue Computations: Theory*, Classics in Applied Mathematics. Society for Industrial and Applied Mathematics: Philadelphia, PA, 2002.
20. Bennighof JK, Kaplan MF. Frequency window implementation of adaptive multi-level substructuring. *Journal of Vibration and Acoustics* 1998; **120**(2):409–418.
21. Abaqus Standard, Version 6.11, Dassault Systems Simulia Corp, 2011.
22. ISO-2631. *Guide for the Evaluation of Human Exposure to Whole-Body Vibration*. International Organization for Standardization: Geneva, Switzerland, 1974.

DOI: 10.1002/nme